Peptide Grafted Poly(Ethylene Glycol) Hydrogel as Biomaterial for Endothelial Colony Forming Cells

by

Wen Jun Seeto (Aaron)

A thesis submitted to the Graduate Faculty of
Auburn University
in partial fulfillment of the
requirements for the Degree of
Master of Science

Auburn, Alabama
Aug 4, 2012

Keywords: Hydrogels, Endothelial Progenitor Cells

Approved by

Elizabeth A. Lipke, Chair, Assistant Professor of Chemical Engineering
Mark E. Byrne, Daniel F. & Josephine Breeden Associate Professor of Chemical Engineering
Steve R. Duke, Alumni Associate Professor of Chemical Engineering
Jiangzhong Shen, Assistant Professor of Pharmacology

ABSTRACT

Endothelial progenitor cells (EPCs) have the potential to become a reliable source of autologous cells for endothelialization of intravascular devices and vascularization of tissue engineered constructs. Endothelial colony forming cells (ECFCs) are one type of EPCs; ECFCs have a highly proliferative and differentiative nature and are capable of forming mature and functional endothelial cells for vessel repair and postnatal angiogenesis. However, currently little is currently known about the homing of these circulating ECFCs. This research investigated the rolling of ECFCs on peptide grafted hydrogels using a parallel plate flow chamber in order to mimic the dynamic adhesion of ECFCs under conditions simulating physiological arterial flow. Poly (ethylene glycol) diacrylate (PEGDA) was chosen to be the hydrogel backbone. Due to the ability of PEGDA to inhibit protein adsorption, it can be used as a "blank slate" to examine the specific interactions of cells with the covalently incorporated peptides. To assess the specific interactions required for ECFCs to interact with material coatings under shear, peptides including RGDS, REDV, YIGSR, and RGES were coupled to acryloyl-PEG and grafted onto the surface of PEG hydrogels. To study the effect of shear on cell rolling, the ECFC cell suspension was sheared over the hydrogels at rates of 20 s^{-1}, 40 s^{-1}, 80 s^{-1}, and 120 s^{-1}. ECFC rolling was significantly lower on REDV-grafted hydrogel. Migration experiments were also performed to examine the migration capability of ECFCs on the

hydrogel surfaces. These results can be applied in the future for modification of biomaterial surfaces to enhance endothelialization.

ACKNOWLEDGMENTS

I would like to thank my advisor, Dr. Elizabeth Lipke, for her guidance and support throughout my research. I would also like to thank my committee members, Dr. Mark Byrne, Dr. Steve Duke, and Dr. Jianzhong Shen for their time and knowledge in the preparation and critical review of this manuscript. In addition, I would like to thank Dr. Mike Meadows and Dr. Yonnie Wu for providing advice on NMR and Mass Spectrometry. I would like to give special thanks to Stephen Hicks who has been my greatest partner since the start of the lab. I would also like to acknowledge the help of my colleagues Dr. David Dunn, Alex Hodge, Sam Chang and Shantanu Pradha. I would like to express my appreciation to Dong Chen and Isabel Tian for doing research together.

Most importantly, I express gratitude to my uncle, William Sun, my aunt, Berginia Lee-Sun and my cousins, Nikke Sun, Mani Sun and Orion Sun, who have loved me so much during my time in the US. I would also like to thank Brian Lilly for enriching my life with indelible memories at Auburn University. I am extremely grateful to Teng Xu for her greatest support and love for me. Lastly, I would like to thank my friends at Auburn, especially Qiang Gu, Rui Xu, Sihe Zhang, Ying Zhu, Yixian Yang, Jingran Duan, Suan Shi.

The bibliography was prepared in the style of Annual of Biomedical Engineering. Microsoft Word, Microsoft Excel, Microsoft PowerPoint, Microsoft Visio, Matlab, ChemSketch, and Google Sketchup were used to prepare this manuscript.

TABLE OF CONTENTS

LIST OF FIGURES

LIST OF TABLES

LIST OF ABBREVIATIONS

6HRGDS	HHHHHHRGDSG
AHA	American Heart Association
bFGF	Basic fibroblast growth factor
BMS	Bare metal stent
BSA	Bovine serum albumin
C=C	Carbon---carbon double bond
CABG	Coronary artery bypass grafting
CAD	Coronary artery disease
CB-EPC	Umbilical cord blood derived EPC
CFU	Colony-forming unit
CVD	Cardiovascular diseases
DES	Drug-eluting stent
DMPA	2,2-dimethoxy-2-phenylacetophenone
ECFC	Endothelial colony forming cells
EPC	Endothelial progenitor cell
FDA	Food and Drug Administration
HSC	Hematopoietic stem cell
KOH	Potassium hydroxide
LDL	Low-density lipoprotein
LST	Late stent thrombosis
MI	Myocardial infarction
MNC	Mononuclear cell
MW	Molecular weight
NMR	Nuclear magnetic resonance
PAD	Peripheral artery disease

PCI	Percutaneous coronary intervention
PEG	Poly(ethylene glycol)
PEGDA	Poly(ethylene glycol) diacrylate
PES	Paclitaxel-eluting stent
PVD	Peripheral vascular disease
SES	Sirolimus-eluting stent
SMC	Smooth muscle cell
ST	Stent thrombosis
SVA	Succinimidyl valerate
TLR	Target lesion revascularization
TRIAS	TRI-stent Adjudication Study
VEGF	Vascular endothelial growth factor

1. INTRODUCTION

For years, cardiovascular disease (CVD) has been a major cause of death worldwide, and 82 million American adults have CVD according to the 2012 statistical update by the American Heart Association (AHA) [61]. Atherosclerosis is one of the most common forms of CVD. In atherosclerosis, a patient's blood vessel wall, typically an artery, is thickened by the buildup of plaque. This results in the narrowing of the blood vessel lumen and thereby restricts blood supply to the body. When atherosclerosis occurs in an artery of the heart, heart attack could occur and the result could be fatal. In these cases, surgical treatment is necessary to physically restore the blood supply.

Angioplasty coupled with stenting is the most common and efficient surgical procedure to treat a narrowed vessel. In this procedure, a balloon catheter is inflated to physically open the narrowed vessel and a stent is placed to keep the vessel from collapsing. Bare metal stents (BMS) were first approved for use in 1994 in the US. Several other designs have been subsequently developed to improve their flexibility and ease of surgical use. However, result of clinical studies have shown that 20-25% of the patients with implanted BMS have restenosis, or re-narrowing of the blood vessel, six months after surgery. This is due impart to the over proliferation of smooth muscle cells (SMCs) which is known as neointimal hyperplasia [31]. To prevent the growth of SMCs, pharmaceutical companies have developed drug-eluting stents (DES) which release drugs to inhibit cell growth. Unfortunately, in some cases, patients with DES developed a condition called late-stent thrombosis (LST)where a blood clot is formed after all the drug in the DES has been released [77]. Thrombosis often causes myocardial infarction (MI) or even death in some situations, and the cause of thrombosis has been determined

to be the inability of the vessel to reform the endothelium while the drug is being released. Endothelium serves as a lining for blood vessels to prevent neointimal hyperplasia. To more rapidly re-form a functional endothelium, the Genous stent was developed. This stent is designed so that the surface of the stent can capture endothelial progenitor cells (EPCs). Nevertheless, several studies have shown that the Genous stent also causes late lumen loss, which is defined as the decrease in minimum lumen diameter. This is due to the fact that the stent not only captures EPCs, but also other cell types [21]. Therefore, endothelium did not re-form completely over the surface of the stent.

In order to achieve complete endothelialization, a better understanding of EPCs is critical for stent design. The purpose of this study is to further characterize the capture mechanism of EPCs to a substrate by engineering a biomaterial that has potential in restoring a functional endothelium. Hydrogels were chosen in this study due to a variety of advantages, such as high water content, the ability to undergo polymerization under physiological conditions, ease of modification, and tailorable mechanical properties. Peptides were used to functionalize the surface of the hydrogel in order to provide a cellular responsive platform for EPCs to adhere to and proliferate. A flow chamber setup and software tracking system were developed to characterize the rolling of EPCs under flow and the effect of using a peptide grafted hydrogel. A custom migration assay was also developed to study the migration of EPCs on the surface of the hydrogel.

The results of this work are important to the development of "next generation" stent materials capable of supporting EPC capture. First, this study demonstrates the potential of using EPCs as the cell source in re-forming functional endothelium to prevent restenosis. This approach more closely mimics human physiology as compared

to the use of current DES where endothelium may never be re-formed in the target vessel locations. Second, this study is intended to realize the potential of using hydrogels as the base stent scaffold material instead of traditional materials like stainless steel. Finally, the developed cell tracking system and migration assay allows us to further advance our understanding of EPC biology or behaviors under physiological flow. The knowledge gained in this work could be more generally applied to biomaterial design in order to enhance EPC capture and migration.

2. BACKGROUND

2.1 Stenosis

Stenosis is a vascular disease where narrowing of blood vessels occurs. The blood vessel narrowing causes restriction of blood flow and reduces the supply of nutrients and oxygen to the body. Stenosis can theoretically occur in any blood vessel. When it occurs in a coronary artery, this refers to coronary artery disease (CAD). Similarly, a stroke may result in patients having carotid artery disease when there is a narrowing in carotid artery. The narrowing of vessels in the other parts of the body is called peripheral vascular disease (PVD). One specific type of PVD is peripheral artery disease (PAD).

One of the most common forms of stenosis is atherosclerosis, which refers to the constriction of blood flow and is caused by a buildup of plaque in the arterial wall. Plaque formation is initiated during an inflammation process where low-density lipoprotein (LDL) cholesterol initially accumulates within the artery wall, followed by the attachment of lipid-laden monocytes, macrophages, and leukocytes as a result of an immune response. Smooth muscle cell migration into the area results in the formation of a fibrous cap. Hence, the artery wall is thickened and hardened. The fibrous cap covers the cells and lipids underneath, eventually making the tissue necrotic and leading to plaque formation. In PAD, this plaque formation may cause a number of adverse effects due to reduced blood supply. When gangrene sets in and amputation of limbs is sometime necessary. In addition, the plaque may rupture resulting in thrombosis. When the thrombus is separated and falls into the blood stream, blockage of smaller vessels

may result causing ischemia, tissue damage, and possibly death. Therefore, atherosclerosis is very dangerous.

Atherogenesis is the development of atherosclerosis and is not yet completely understood. The hypothesis was first made that the endothelium was denuded, allowing the lesion site to accumulate lipid [63], but later there was another hypothesis suggesting that endothelium dysfunction is the initial step [62]. When the function of the endothelium is compromised, the adhesiveness and permeability to leukocytes or platelets is increased which initiates the buildup of plaque. There are multiple risk factors that affect the endothelium including elevated LDL level, smoking, hypertension, diabetes, genetics, plasma homocysteine concentrations, and infectious microorganisms. Hence, the mechanism of atherogenesis remains to be exclusively determined.

Surgical treatment is necessary when stenosis or atherosclerosis cannot be controlled by change of life style or medication. The most common treatment is percutaneous coronary intervention (PCI), also known as balloon angioplasty or simply "angioplasty". In PCI, a guide wire is used to move a balloon catheter through blood vessel and the balloon catheter is inflated at the site of stenosis to open up the narrowed vessel. Coronary artery bypass grafting (CABG) is another option in restoring blood supply. Although studies have shown that CABG has the advantage of lower death and myocardial infarction rates, angioplasty is more common due to several reasons. CABG is a more invasive surgery comparing to angioplasty, surgical risk and cost are much higher than angioplasty. In small diameter vessel grafting, the grafts usually have limited lifespan and causing rapid occlusion. In addition, CABG uses autologous artery from other part of the body to restore blood flow, 60% of patients with vascular disease do not

have suitable vessel for autografting [67]. Also, due to the fact that As a result, patients have a much slower recovery and more discomfort. Therefore, angioplasty is a more common treatment in terms of improving the quality of life.

2.2 Stents

In the 1970's, some patients who underwent angioplasty experienced immediate collapsing or negative remodeling of their arteries, so stents were developed to be used to correct this issue. Depending on the artery size and blockage location, stents are now often used together with angioplasty to prevent the artery from collapsing. However, there are other complications associated with the use of stents due to the material design of stents. This section will elaborate several main points.

2.2.1 Bare Metal Stents

The BMS is the first generation stent developed to prevent the artery from collapsing after angioplasty. The first BMS that was approved by Food and Drug Administration (FDA) was the Palmaz-Schatz stent in 1994. This stent is a metal mesh wire tube which is expandable upon inflating the balloon catheter and stays expanded within the artery. The BMS had success in increasing the luminal diameter following placement and maintaining a larger luminal diameter six months after treatment comparing to balloon angioplasty [18,72]. Comparing to angioplasty, patients with BMS implantation have a decreased rate of target lesion revascularization (TLR) which is defined as any repeat revascularization procedure of the original target lesion site [41]. However, in-stent restenosis occurred in some patients. According to a study by Hoffmann *et al.*, 37% of lesions treated with BMS were restenotic at follow-up six months after stent implantation and required repeat treatments. They concluded that

neointimal tissue proliferation contributed to in-stent restenosis [31]. On the other hand, the outcome of stenting procedures may also be influenced by the geometric design of the stent. For example, a study has shown that slotted-tube stents may have a significantly lower rate of restenosis than coiled stents as determined at a six-month follow-up [56]. Therefore, solutions are needed to prevent neointimal tissue proliferation and therefore avoid in-stent restenosis with the BMS.

2.2.2 Drug-Eluting Stents

The DES were invented to provide a solution to prevent the neointimal proliferation that was frequently found in patients using BMS. DES are simply BMS with coatings that release drugs which inhibit cell growth. Although there are various types and numbers of layers of coatings, the fundamental design of DES are very similar. There are usually two coatings consisting a polymer coating that releasing the drug and another coating that keeps the drug releasing layer on the stent. In some designs, a third coating exists on top of the outer layer to slow down drug release. The most common drugs being released to inhibit neointimal proliferation are Sirolimus and Paclitaxel. Everolimus, which is a derivative of sirolimus, and heparin are also used in some clinical studies. This section describes some of the characteristics and drawbacks of DES which motivates the development of EPC capture stents.

Sirolimus-eluting stents (SES) release sirolimus, also known as rapamycin, which is an immunosuppressant drug used to prevent rejection in organ transplantation. Paclitaxel-eluting stents (PES) release paclitaxel, which is a mitotic inhibitor used in cancer chemotherapy. Both drugs are able to be released from a polymer system coated on DES to inhibit cell growth. Patients with DES are required to be pretreated with anti-

platelet therapy in order to prevent stent thrombosis. Pre-treatments prior to stent placement include ticlopidine or clopidogrel and aspirin. After implantation, aspirin was continued indefinitely, and ticlopidine or clopidogrel is given at least for another 3 months for SES implantation or 6 months for PES implantation respectively.

From a world-wide pooled analysis with respect to four trials (RAVEL, SIRIUS, E-SIRIUS, and C-SIRUIS) comparing SES to BMS and five trials (TAXUS I, II, IV, V and VI) comparing PES to BMS, a reduced TLR was shown after 4 years in both DES comparing to BMS. However, DES caused stent thrombosis (ST) and delayed neointimal proliferation. According to an observational cohort study on stent implantation between April 2002 and January 2004, there was a higher number of ST events in both SES and PES than in BMS after both 1 and 4-year time points, where ST was found in 29 patients with either SES or PES at 9-month follow-up and caused 13 deaths[77]. On the other hand, Carter *et al.* performed an *in vivo* study using porcine model where histological analysis found a delayed neointimal proliferation using SES and the result was similar to BMS at day 90 and 180 [11]. From these results, DES and anti-platelet therapy have not only inhibited the cell proliferation that causes restenosis, but also the re-formation of the endothelium which is critical in preventing thrombosis. Thrombosis can cause acute blockage of arteries and lead to myocardial infarction which is fatal. Therefore, alternatives to promote endothelialization of the target stent are desired.

2.2.3 EPC Capture Stents

The presence of the endothelium seems to be essential to eliminate the issue of in-stent thrombosis and restenosis. As a result, an EPC stent has been developed with the goal to re-endothelialize the stent with patient's own EPCs that captured from their

circulating blood. Figure 1 shows an EPC stent with an anti-CD34 antibody presents on the surface of a metal stent; this antibody is responsible for capturing EPCs that have been found to be CD34+. After the implantation of the EPC stent, circulating EPCs bind and cover the surface of the stent in order to re-form the endothelium. Although clinical results showed some improvements over DES, patients still develop complications. In a single-center TRI-stent Adjudication Study (TRIAS) that has 193 patients, a higher rate of late lumen loss, which is a delayed reduction in minimum vessel diameter, was reported as compared to patients using the Taxus stent [7]. In HEALING-IIb clinical trial that has 100 patients, the in-stent thrombosis rate was found to be 3% at 12-month follow-up and two patients died due to acute in-stent thrombosis within the first 30 days. In the GENIUS-STEMI study that has 100 patients, there was a 6% stent thrombosis rate in patients treated with the EPC stent whereas the rate of ST was 0% in patients treated with BMS. Also, Rossi *et al.* reported that ST and restenosis occurred in one patient after clopidogrel was stopped [64]. In summary, the efficacy of the EPC stents remains uncertain.

There are two widely acceptable explanations for these results. The first explanation is that the EPC stent may not be capturing EPCs exclusively. Although EPCs were historically defined as CD34+ cells, CD34 is also expressed by some other mesoderm progeny including blood cells, ECs, fibroblasts, epithelial lineage, and cancer stem cell populations [30]. Studies have shown that only 0.4% of CD34+ cells are actually EPCs, so the EPC stent is probably primarily capturing other cells types that do not contribute in endothelialization[57]. The second explanation is that the cells captured did not differentiate into ECs. The CD34+ cells possess the ability to differentiate into other

cell types such as cardiomyocytes and vascular SMCs [73,74,92]. Therefore, the captured cells may differentiate into vascular SMCs which are known to hinder the endothelialization process and contribute largely to late lumen loss and ST. As a result, the lack of knowledge in EPC biology created a design flaw in the current EPC stent leading to less than desired clinical result.

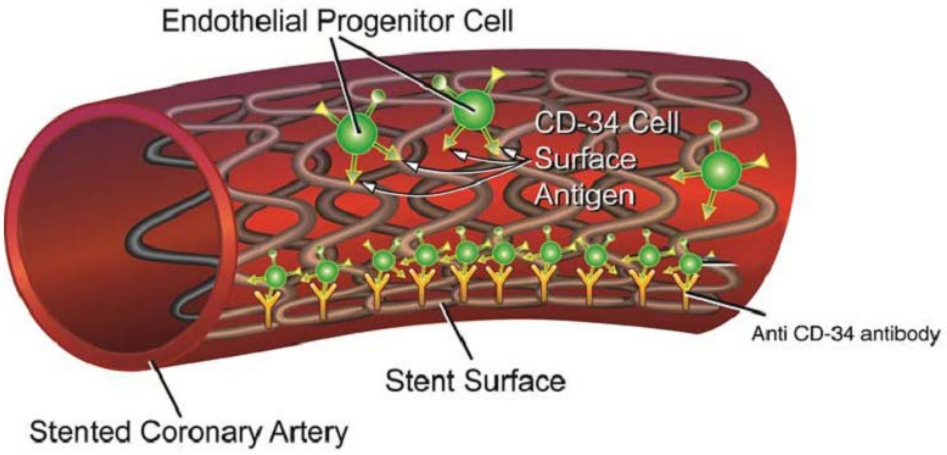

Figure 1: The Genous EPC stent. The Genous EPC stent has anti-CD34 antibody which is immobilized on the surface of a metal stent which is responsible for capturing the patient's own EPCs through the binding of the CD34 antigens on their EPCs. Reprinted with permission from Ref 21.

2.3 Endothelial Progenitor Cells

In the field of regenerative medicine, more evidence has been shown in using EPCs as a potential candidate for tissue repair since their discovery [4]. As a precursor for endothelial cells (ECs), EPCs show an endothelial-like phenotype and can be differentiated into mature endothelial cells that form the endothelium. Hence, potential clinical applications of EPCs include vessel repair [4], neovascularization of ischemic organs, and coating of vascular grafts [32]. This section provides more details of EPCs characterization and biology.

2.3.1 EPC History and Types

EPCs were discovered by Asahara *et al.* in 1997 who postulated that angioblasts and hematopoietic stem cells (HSCs) exist in circulating adult blood and contribute to vasculogenesis. Since both angioblasts and HSCs share the surface marker CD34, they isolated the CD34+ mononuclear cells (MNCs), which are a type of leukocytes, using magnetic beads coated with the antibody for CD34. After isolating the CD34+ MNCs from adult blood, they found that the CD34+ cells were able to form cellular networks and tube-like structures on fibronectin-coated plates. Furthermore, using ischemic hindlimb model in both mice and rabbits, CD34+ MNCs were able to incorporate into capillary vessel walls of whereas CD34- MNCs did not. Although later studies have shown that not all CD34+ cells are EPCs, these cells do possess proangiogenic capabilities and contribute to neoangiogenesis.

Other than CD34, EPCs generally co-express the surface markers AC133 and VEGFR-2 (or KDR) [6,57,94], and they can be separated into two types: early and late outgrowth EPCs. Different methods are used for isolating early and late EPCs [30,94]. The early EPCs or colony forming units (CFUs) are isolated by first seeding MNCs onto fibronectin-coated plates and, after 48 hours, the nonadherent cells are then replated. At day 5 to 7, CFU colonies are identified as elongated sprouting cells. On the other hand, the late EPCs, which are ECFCs, are isolating by first seeding MNCs on collagen-coated plates, and the nonadherent cells are then discarded. After 1 to 2 weeks, ECFCs colonies are identified based on their cobblestone morphology [5,30,94]. It remains in question whether the CFUs and ECFCs are derived from the same parent cell, but Yoder has reported that the CFUs are clonally distinct from ECFCs using clonal analysis [94]. They

determined that both CFUs and ECFCs express endothelial antigens including CD31, CD105, CD144, CD146, vWF, KDR, and UEA-1, but only CFUs express the hematopoeitic-specific cell surface antigen, CD45, and the macrophage cell surface antigen CD14, and CD115 [94] (Table 1). This proves that CFUs are derived from HSCs, whereas ECFCs are not derived from HSCs. Furthermore, CFUs were shown to function as macrophages and did not possess the ability to form vascular structures *in vivo*. On the other hand, ECFCs formed functional human-murine chimeric vessels *in vivo*. Therefore, based on the phenotypic and functional properties of ECFCs, Yoder *et al.* have determined ECFCs to be the true EPCs [30,94].

Table 1: Cell surface antigen expression and Ac-LDL uptake by CFUs and ECFCs Adapted from Ref 94.

Antigen	CFU-ECs	ECFCs
CD31	92.31 ± 5.47	92.29 ± 1.32
CD105	74.36 ± 6.32	96.73 ± 1.79
CD144	34.80 ± 8.74	99.15 ± 0.85
CD146	56.52 ± 10.00	94.21 ± 3.71
KDR	99.19 ± 0.81	68.61 ± 11.26
vWF	67.21 ± 12.78	97.09 ± 2.05
Ac-LDL	73.68 ± 9.05	99.75 ± 0.25
CD14	98.53 ± 1.04	1.20 ± 0.74
CD45	98.15 ± 1.85	0.37 ± 0.37
CD115	94.42 ± 2.52	0.28 ± 0.21

2.3.2 Advantage of EPC as Cell Therapy

Aside from the clinical outcome and safety issues of Genous EPC capture stent, the idea of implementing EPCs for stent endothelialization as a preventative for restenosis remains robust. Although ECFCs are the main focus in this study, both types of EPC are have been shown to contribute equally to endothelialization through separate

mechanisms. CFUs enhance angiogenesis through secretion of angiogenic cytokines to induce survival and proliferation of mature endothelial cells. Due to their highly proliferative capability, ECFCs contribute by providing a relevant number of endothelial cells [37]. EPCs have advantages over ECs for cell therapy, since mature ECs have low proliferative potential and limited ability to regenerate damaged endothelium. Most importantly, autologous EPCs are readily obtainable from the blood comparing to mature ECs which would be isolated from tissue. The number of ECs in circulating blood is very low and they are commonly damaged ECs that have shed off from the vessel wall [50], so patients' circulating ECs are not suitable for re-endothelialization. In addition, EPCs have also been shown to be a strong candidate for endothelialization due to the fact that they can withstand superphysiological shear stress up to 250 dyn/cm [29,78]. They have been seeded on Ti surfaces for implantable devices to prevent thrombosis in a porcine model [1,38]. Therefore, EPCs are an excellent source for cell therapy to promote rapid endothelialization. Figure 2 shows a schematic that summarizes the idea of implementing EPCs in cell therapy with the use of biomaterials like hydrogels.

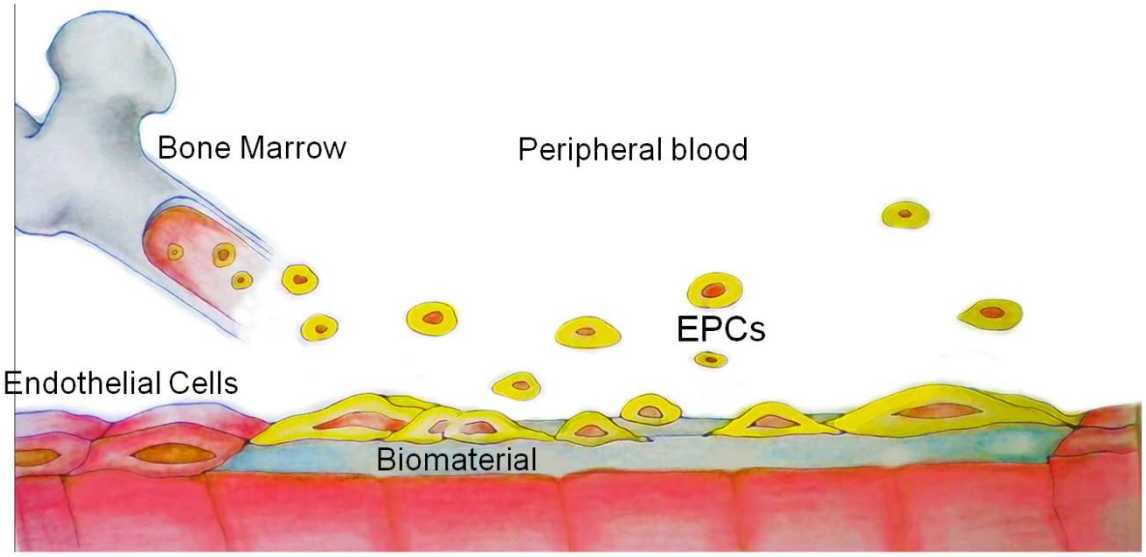

Figure 2: Schematic of using EPC capturing biomaterial for vessel repair. The ultimate goal of this study is to develop a EPC specific hydrogel as biomaterial to capture EPCs and support EPC rolling, adhesion, and migration for endothelialization of injured vessel. Illustration by Isabel Tian.

2.4 Hydrogel

Hydrogels are a network of polymer chains forming a hydrophilic scaffold and are widely studied and used in tissue engineering due to their various advantageous properties. Since hydrogels are very hydrophilic, they absorb water and swell to form a very flexible material that is similar to natural tissue. Most precursor polymers can form hydrogels under physiological pH and temperature. Synthetic hydrogels are highly reproducible materials that reduce the variability from batch to batch possessed by natural material, like ECM protein. Hydrogels can also be easily modified with natural materials to form hybrid scaffolds for different purposes. They play a key role as an interfacial biomaterial for various applications including drug delivery, microencapsulation, coatings for vascular grafts, and diagnostic devices [58,75].

Poly(ethylene glycol) (PEG) is a very unique synthetic polymer that forms PEG hydrogels with excellent properties for use in tissue engineering. It is well known for its biocompatibility and minimal protein adsorption due to the steric hindrance by water absorbed [29]. In other words, it is non-thrombogenic and non-inflammatory due to high resistance in platelet and macrophage adhesion. Molecular weight (MW) of PEG was found to affect the cytotoxicity where MW less than 400 is cytoxic due to oxidation of PEG *in vivo* forming diacid and hydroxyacid metabolites [28], and a MW of 1,000 or above have been proved to be safe [91]. Therefore, the PEG that are chosen in this study have a molecular weight of 3,400 and 6,000.

PEG is acrylated to form poly(ethylene glycol) diacrylate (PEGDA) before possessing the ability to crosslink into hydrogel. This also provides the capability in the functionalization of the PEG hydrogel. The crosslinking is a rapid photopolymerization process adapting a free radical chemistry together with photoinitiator and long wavelength ultraviolet light. The chemical structure of PEGDA is shown in Figure 3. PVA is another major synthetic polymer in forming hydrogel that can be crosslinked using physical, chemical or irradiative methods, but these methods may be time consuming comparing to the photopolymerization of PEGDA [52,53,59,68].

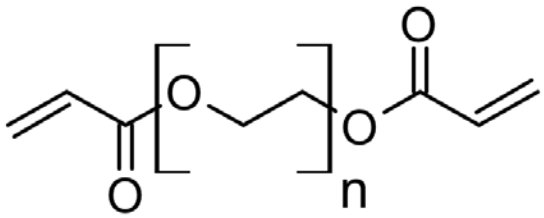

Figure 3: The chemical structure of poly(ethylene glycol) diacrylate (PEGDA). Figure was drawn using ChemSketch.

2.4.1 Hydrogel as Potential Biomaterial for ECFCs

Hydrogels have advantages in serving as biomaterials to capture EPC over traditional metal stents. *In vivo* studies have shown that hydrogel can be crosslinked and formed *in situ* within blood vessel simply by injection of polymer precursor solution and UV radiation through the skin [88]. This significantly reduces the need for invasive surgery and decreases the complexity of surgery. Unlike metal stents, it can be instantaneously produced due to the rapid crosslinking by photopolymerization. Quality of the material can be achieved by the decrease in batch-to-batch variability due to the intrinsic property of synthetic polymer. Therefore, hydrogel provides an alternative for metal stents.

2.4.2 NMR in Characterizing PEG Acrylation

PEG is reacted with acryloyl chloride to form PEGDA and the extent of PEG acrylation is determined in order to verify the success of PEG acrylation. Proton nuclear magnetic resonance (NMR) is a common method in determining the extent of PEG acrylation [19,25,27,48,84]. Protons of a molecule undergo chemical shift due to the magnetic field supplied by NMR, and this chemical shift, that is reported in ppm, is used to diagnose the structure of the molecule. Peaks representing the protons on the acrylate group are typically found around 6.00, 6.20, and 6.45 ppm where the peak for protons on the PEG is commonly found around 3.70 ppm. After identifying the peaks, integrated intensity of each proton is estimated by integration of the areas under the peaks since the areas reflect the abundance of the individual protons. Deuterium oxide is used as solvent to avoid interference to the protons in the sample.

2.4.3 PEGDA Crosslinking/Free Radical Chemistry

PEGDA is crosslinked into hydrogel networks by photopolymerization using photoinitiator, and photopolymerization consists of the initiation, propagation, and termination steps. There are three major types of photoinitiation: photocleavage, hydrogen abstraction, and cationic photopolymerization [51], where photocleavage is one of the most commonly used approach in crosslinking PEGDA. As an example of photocleavage shown in Figure 4, 2,2-dimethoxy-2-phenylacetophenone (DMPA) is a photoinitiator where a methyl free radical $CH_3\cdot$ is generated when DMPA is exposed to UV light. Then, the methyl radical attacks the carbon-carbon double bond (C=C) in the acrylate groups of PEGDA to form $CH_2\cdot$ on PEGDA. Hence, the $CH_2\cdot$ propagates to other PEGDA until termination of the reaction [47]. Figure 5 shows the propagation of PEGDA after being attacked by the methyl radical. Other than the concentration of PEGDA and photoinitiator used, the crosslinking time needed also depends upon the choice of photoinitiator and the power of the UV light. Take DMPA as an example, it varies from 3 s under 20 W/cm^2 to 30 min under 1 W/cm^2 [47,71].

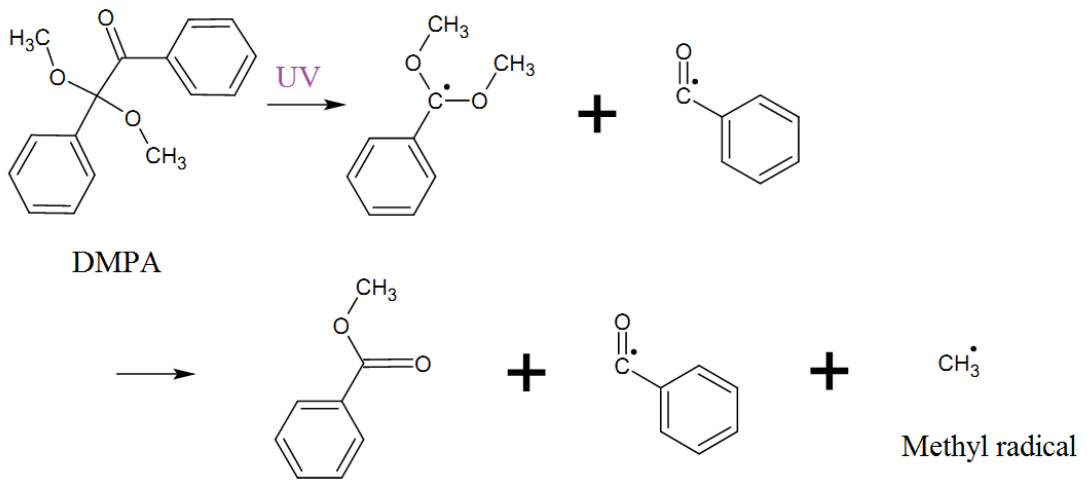

Figure 4: The photoinitiation of DMPA started by exposure to UV light to generate reactive methyl free radical. Figure was drawn using ChemSketch.

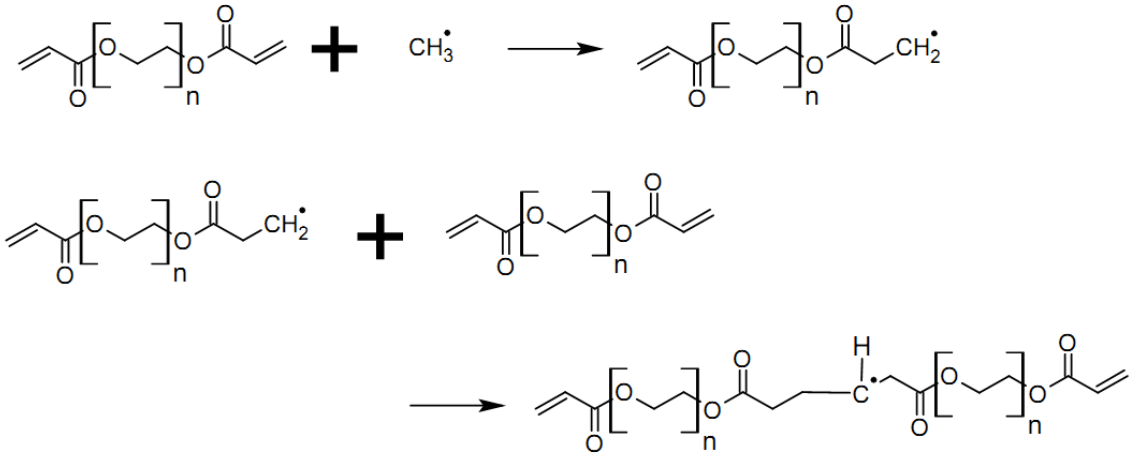

Figure 5: The propagation of PEGDA by reactive methyl free radical generated by DMPA under exposure to UV. Figure was drawn using ChemSketch.

2.4.4 Photoinitiator Selection

DMPA has been selected as the photoinitiator in this study. There are four major choices of photoinitiators that are seen frequently in literature in crosslinking PEGDA, and they are 1-Hydroxy-cyclohexyl-phenyl-ketone (I-184), I-651 (which is DMPA), 1-[4-(2-Hydroxyethoxy)-phenyl]-2-hydroxy-2-methyl-1-propane-1-one (I-2959), and eosin Y. DMPA is the one that is selected and implemented in this study due to its superior

performance at the wavelength of 365 nm comparing to I-184 and I-2959, as shown in Figure 6, where 365 nm is within the Food and Drug Administration (FDA) approved wavelength. I-2959 has been shown in study with cell encapsulation due to the minimal effect in cell viability, but it is only strongly sensitive to 305 nm light [90]. This wavelength is not FDA approved because it falls into the mutagenic UVB spectrum. Therefore, it is not the best option to work with. Eosin Y is also proved to have minimal effect on cell viability and it is readily able to crosslink PEGDA from 450 nm to 550 nm. However, it also serves as a cytoplasmic stain with green fluorescence, so it may interfere with immunostaining. Although DMPA has cell viability issues, cell viability should not be a concern since cells were only come in contact with the hydrogel after the polymer precursor is crosslinked and swollen.

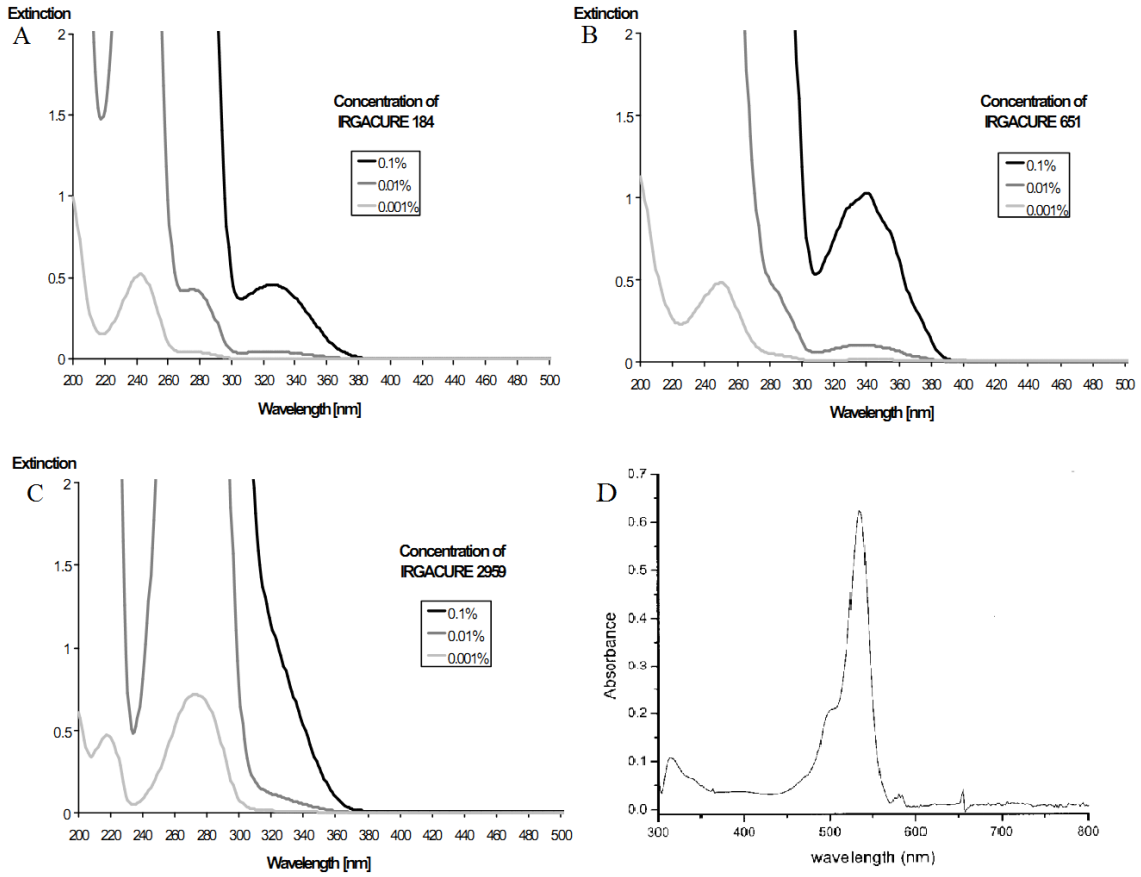

Figure 6: Absorbance spectrum of I-184, I-651, I-2959, and eosin Y. (A-C) Reprinted from specification data sheet. (D) Reprinted with permission from Ref 54.

2.5 Integrins

2.5.1 Integrin Structure

Integrins are a family of proteins present on the cell surface that play a key role in cell adhesion. An integrin is a heterodimeric protein that has an α and a β subunit where 19 α and 8 β subunits have been discovered in mammals [36]. Specificity of integrin binding is determined by the different combination of the α and β subunit. Figure 7 shows the known integrin subunit combinations [65]. Although integrins also possess signal transduction ability in modulating numerous cellular activities that affect cell

proliferation and differentiation [12,23], their role in cell adhesion is the primary concern in this study in terms of cell rolling and migration.

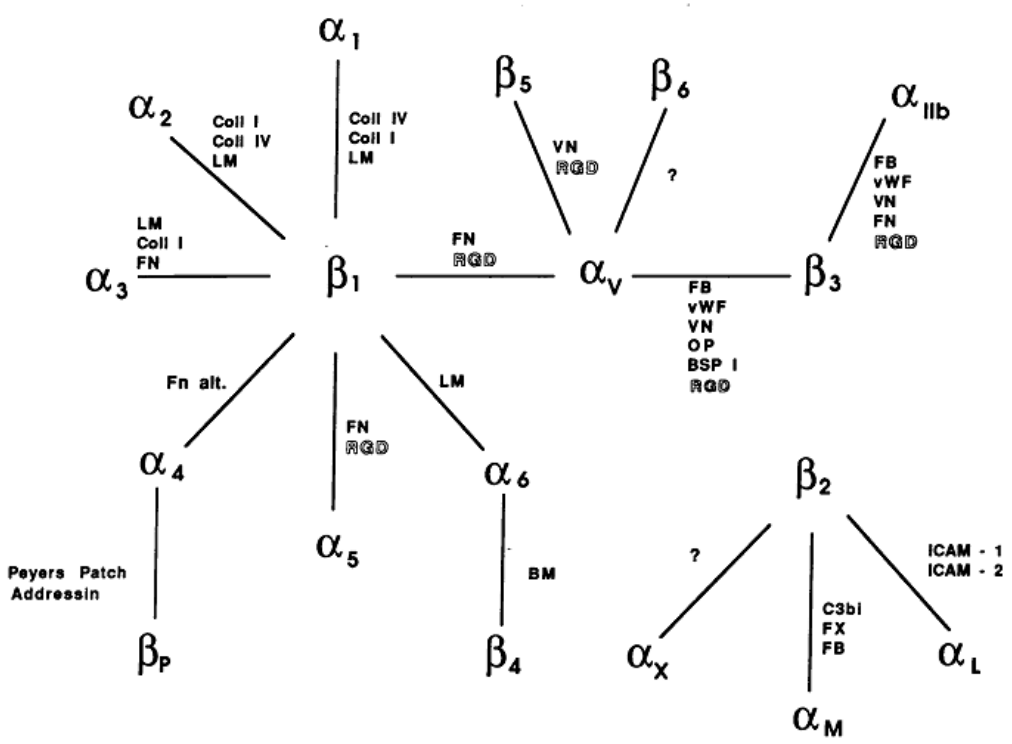

Figure 7: Integrin map showing the combinations of α and β subunits, and their ligands Reprinted with permission from Ref 65. This article Copyright © 1991, The American Society for Clinical Investigation.

2.5.2 Integrins Found on EPCs

Some recent studies have explored the involvement of integrins in adhesion. *In vivo* studies have shown that β_2 integrins are important in both EPC homing to site of ischemia and neovascularization [13]. Integrins also play an important role in EPC arrest on EC or ECM proteins *in vitro* [33]. Although the types of integrin receptors are not well identified on EPC, Angelos *et al.* have estimated the number of $\alpha_5\beta_1$ and $\alpha_v\beta_3$ integrin receptors present on umbilical cord-blood derived EPC using flow cytometry [3]. Besides

flow cytometry, study of EPC migration has shown that $\alpha_5\beta_1$decreases EPC migration when the $\alpha_5\beta_1$integrins are blocked [89]. Until now, knowledge of integrin on EPC is still very limited and needed to be explored.

2.6 Peptide

The study and use of peptides as a biomaterial has been growing rapidly because they possess excellent advantages over proteins. Unlike ECM proteins, peptides are able to be synthesized in a very defined manner, so this allows the identification of the critical peptide sequence within a protein as a specific ligand. On the other hand, more and more novel peptides that are specific to their receptors have been discovered which leads to a better understanding of the role of these receptors in cellular activities. Also, with the improved technology in peptide synthesis, the batch-to-batch variations that commonly occur in protein production is very minimal in peptide production. Therefore, peptide is chosen in this study as biomaterial to study ECFCs homing due to its great potential.

2.6.1 Peptide Structure

A peptide is a short sequence of amino acids joined by peptide bond. Depending on the sequence of the amino acids, a peptide may or may not be recognized by the integrins. As an example, the amino acid sequence RGD is recognized by half of the over 20 known integrins [66] whereas the sequence RGE has been shown to be not recognized by any integrins. Moreover the length of the peptide may alter the availability of the active portion of the sequence. Most of the short peptides are considered linear and longer peptides are not, and this is due to the tendency of longer peptides to form secondary structure. For example, a bend within a longer peptide occurs when there is a

formation of hydrogen bond or disulfide bond. Therefore, peptide sequence is critical in terms of providing specificity for ligand-receptor recognition.

2.6.2 Peptide Selection

Three major peptides were used for rolling and migration in this study and their structures are shown in Figure 8. The first one is RGDS, which is a peptide that is widely used in tissue engineering as a cell adhesion ligand because it is well recognized by many integrin receptors [66]. It presents in various ECM proteins including fibronectin, vitronectin, laminin, and collagen [87]. Since RGDS is known to bind to $\alpha_v\beta_3$, it has been used to serve as an imaging probe for $\alpha_v\beta_3$ [16,70]. YIGSR is well known to enhance migration. It is a sequence on the B1 chain of laminin and it is the minimum sequence that is necessary to bind 67kDa laminin receptor [26]. Furthermore, YIGSR is often used for promoting endothelialization [22,40], EC adhesion, and spreading [40]. Research has shown that YIGSR modified PEG/PUU gels support EC adhesion, but not platelet adhesion [39]. Although YIGSR is not an integrin binding peptide, it has great potential as a biomaterial for homing of ECFCs [14]. REDV presents in the III-CS domain of human plasma fibronectin and is shown to be EC specific. Although to a lesser extent, it has been shown to promote EC adhesion and spreading [35,46]. Research has shown that it is a potential peptide in capturing ECFCs under flow when REDV is coated in a PDMS microfluidic device [83]. Therefore, these three peptides were chosen to be grafted onto PEG hydrogel for study in ECFCs.

a) 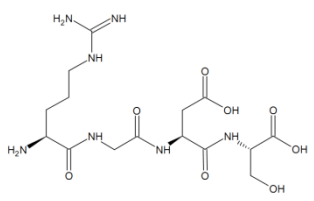 b) 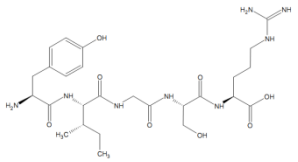 c) 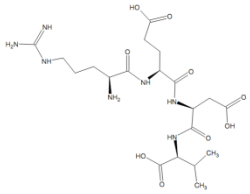

Figure 8: Structure of peptide sequences a) RGDS, b) YIGSR, and c) REDV. Source obtained from Chemicalbook.com

2.6.3 Custom Peptide Synthesis

A custom peptide HHHHHHRGDSG (6HRGDS) was made to characterize the grafting method used in this study. With an automated peptide synthesizer (Apex 396, aapptec, Louisville, Kentucky), one amino acid was added onto a substitution site on a resin at a time by solid phase peptide synthesis. Each resin serves as a base for the building of the peptide with a substitution of 0.55 mmol/g resin. Fmoc/tBu orthorgonal protection scheme was used where the alpha nitrogen is protected with the base labile Fmoc group and the side chains are protected with acid labile group. In other words, the alpha nitrogen and side chain protection groups are removed under completely different pH, so this scheme provides the flexibility in further modification after the peptide is formed. This scheme has another advantage over the Boc protection scheme where undesired peptide product may be formed and multiple washing is required. After the peptide is formed, it is conjugated to the PEG spacer as described in Section 2.6.4.

2.6.4 Peptide Grafting on PEG Hydrogel

Peptides are relatively small molecules comparing to 6 kDa PEGDA, so a PEG spacer arm is incorporated to extend the peptide outward when grafting on the surface of PEG hydrogel. Study has shown that when RGDS with a 3,400 MW PEG spacer arm is used with PEGDA to form hydrogel, endothelial cell spreading has increased

significantly comparing with the ones without the spacer arm [27]. Therefore, the peptides were conjugated to acryloyl-PEG-succinimidyl valerate (acryloyl-PEG-SVA) before grafting. Figure 9 shows the reaction for the conjugation.

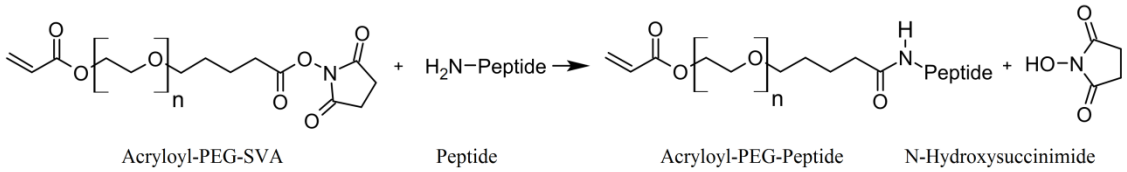

Figure 9: The chemical reaction in conjugating peptide to PEG. Acryloyl-PEG-SVA, a PEG spacer arm, and peptide to form acryloyl-PEG-peptide to extent the peptide outward for better cell adhesion. Figure was drawn using ChemSketch.

Using the free radical chemistry, acryloyl-PEG-peptides were grafted on PEG hydrogel based on the methods seen in several literatures with some modifications [27,49,79]. In the literature, a PEG hydrogel sheet was first formed in between two pieces of glass slides with a 0.5 mm thick spacer to create a PEG hydrogel base. Then the top glass was removed in order to add the acryloyl-PEG-peptide solution with photoinitiator to the top of the base. Next, the top glass was placed again on top of the base and the acryloyl-PEG-peptide was allowed to crosslink to the base. In the preliminary trials, tiny air bubbles were created frequently when placing the top glass on the base with acryloyl-PEG-peptide solution on top. The tiny air bubbles prevented the acryloyl-PEG-peptide to be grafted on the hydrogel. Figure 10 shows that the ECFCs were not able to adhere and grow in the center region where the center region has no RGDS grafted due to the presence of air bubble during crosslinking. Therefore, a slight modification was made to eliminate the creation of bubbles. After the base was formed, the top glass was removed and the 0.5 mm spacer was replaced by a 0.7 mm spacer so that a gap was created between the base and the top glass. Therefore, the acryloyl-PEG-peptide solution can be

injected into the gap and the base can be completely grafted. Figure 11 shows a schematic of peptide-grafted hydrogel.

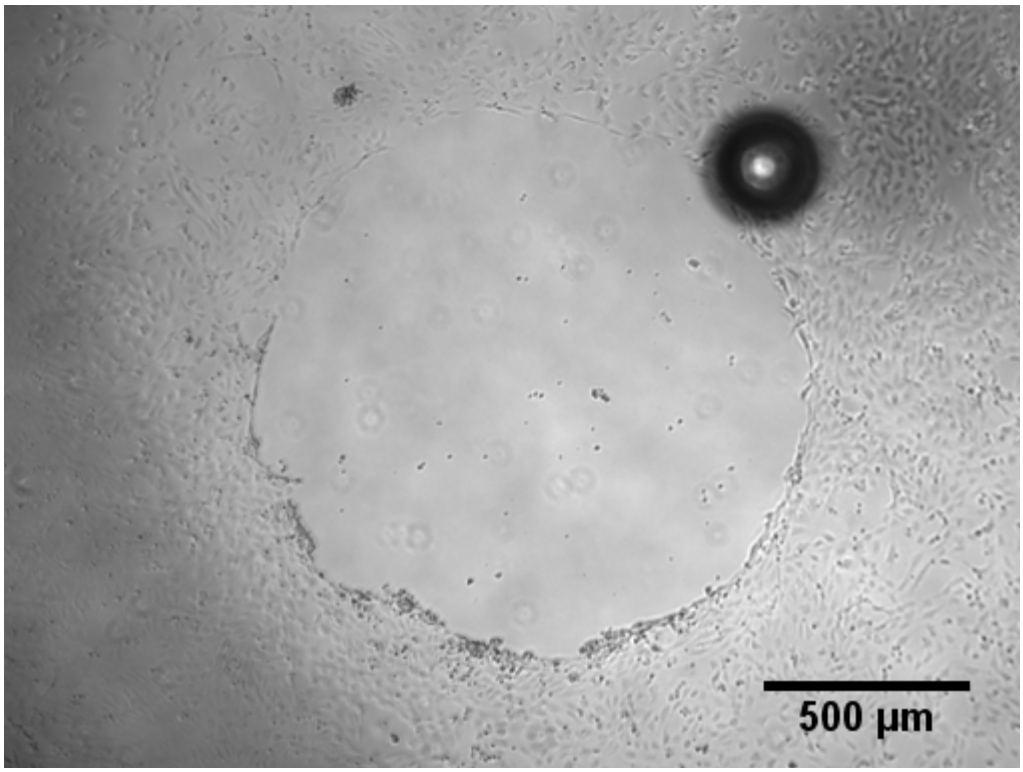

Figure 10: Illustration of incomplete peptide grafting. A tiny bubble was created when re-placing a glass slide on top of a PEG hydrogel with acryloyl-PEG-peptide solution present on the surface. No peptide was grafted on the surface of the PEG hydrogel where the bubble was present, and this was shown by the absence of ECFCs adhesion and proliferation.

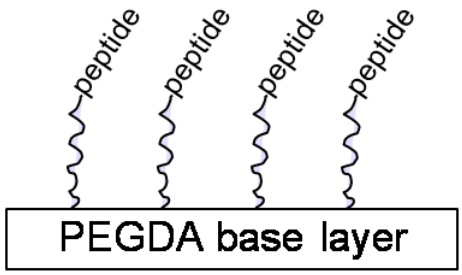

Figure 11: Schematic of peptide-grafted hydrogel. PEGDA was first crosslinked to form the base layer. Then the acryloyl-PEG spacer arm conjugated peptide was dissolved in PBS with photoinitiator and grafted on the PEGDA base layer under UV light.

2.6.5 6x His Tagged Peptide Characterization

Hexahistidine, HHHHHH or 6His, is a peptide that has been used as a tag to indicate the presence of the target component [8,10]. In this study, 6HRGDS was synthesized and used to provide a mean to quantitatively estimate the success of the peptide grafting. First, 6HRGDS was reacted with acryloyl-PEG-SVA to form acryloyl-PEG-6HRGDS and then grafted on PEG hydrogel. An anti-6His-FITC antibody was used in the immunostaining of the 6HRGDS grafted on the surface of the PEG hydrogel. The density of FITC fluorescence probes were read as intensity using a plate reader (Biotek HT). The PEG hydrogel was used as the reference for comparison.

2.7 Blood Vessels Fluid Dynamics

Fluid dynamics in blood vessel is extremely complex, so simplified mathematical models can only be used to aid in understanding the flow in blood vessels. One of the major challenges is due to the fact that blood contains cells, which exist in various sizes, types, and amount. Although blood is generally considered as Newtonian in most arteries,

it appears to be non-Newtonian in the microcirculatory system where low shear rates and clumping of red blood cells occurs. Other than cells, blood contains blood serum which has a large amount of various concentrations and types of proteins where blood viscosity is approximated to be four times of water [42]. Another challenge is the peristaltic nature of blood flow causing the change in diameter of blood vessels. Therefore, the bulk quantities are typically considered to estimate the fluid dynamics for blood vessels. For example, shear rate, shear stress, Reynolds number, and pressure. Reynolds number ranges from 1 in small arterioles to 4000 in largest artery aorta, so blood flow is generally considered as laminar [42]. Since blood vessels are generally considered as tube-like structure, so the equation of Reynolds number for blood vessel is essentially for tubes and is shown in Equation (1) where ρ is the density of the fluid (kg/m^3), v is the average velocity (m/s), D is the diameter of the blood vessel (m), and μ is the viscosity (kg/(m·s)). Similarly, wall shear stress and shear rate of tubes are shown in Equations (2) and (3) respectively. Wall shear stress for most arteries is reported to be approximately 15 dyn/cm^2 [24].

$$Re = \frac{\rho v D}{\mu} \tag{1}$$

$$\tau_{wall} = \frac{32\mu Q}{\pi D^3} \tag{2}$$

$$\dot{\gamma} = \frac{4Q}{\pi r^3} \tag{3}$$

2.8 Parallel Plate Flow Chamber Dynamics

Parallel plate flow chamber has been a standard piece of apparatus in studying the effect of blood vessel like flow on cells [20]. Although the flow geometry is different from

the flow in blood vessels, parallel plate flow chamber has the benefit to provide an easy observation under microscope. The advantage of using parallel plate flow chamber is that it is simple to model and, also, able to capture the fluid-solid interfacial shear phenomenon. It has been used in studying various cell types, such as platelets, leukocytes, epithelial cells, and endothelial cells. Fluid shear can be altered by flow rate, dimension of flow chamber, and viscosity. A fluid pump, like a syringe pump, is commonly used in controlling the flow rate. Gravity driven flow and peristaltic pump are usually applied in cycling flow system for long-term studies. The dimension of a flow chamber is typically controlled by a silicone gasket while viscosity of the fluid is usually determined by temperature and the flow media used. In studies where superphysiological shear stress is necessary, dextran has been used to increase the viscosity of the fluid [9,78]. Detailed characterization of dextran viscosity has shown that the addition of dextran up to 30 wt.% shows Newtonian viscosity behavior [80]. Also, research has shown that 5% dextran did not affect cell expression of Mono Mac 6 cells [60].

The flow chamber setup used in this study was purchased from Glycotech (Gaithersburg, MD). The flow chamber consists of a flow deck, silicone gasket and a flat surface that serves as the bottom plate as shown in Figure 12. The flow deck has the inlet, outlet and a vacuum port. The silicone gasket in light green color defines the width, length and height of the chamber. Hydrogels are placed underneath the flow deck and silicone gasket to serve as the bottom plate of the chamber. Since the flow chamber was initially designed to be used on solid surface that serves as the bottom plate of the chamber, it requires a vacuum to keep the flow deck and silicone gasket to stay firmly on the solid surface. However, hydrogels that were used in this study are too soft in general,

so the vacuum suction deforms the hydrogel sheet and is not able to form a tight seal. Therefore, a modification was implemented to improve the sealing of the chamber. Each piece of hydrogel was first placed on a glass slide. Second, the flow deck and silicone gasket were placed on top of the hydrogel. Third, a PMDS ring was placed around the flow deck and on the glass slide to contain any potential leaks. Lastly, the flow deck, silicone gasket, the hydrogel and glass slide were hold together by using a custom made metal plates and screws as a clamp as shown in Figure 13.

Figure 12: Glycotech flow chamber. Chamber dimension is determined by the silicone gasket in light green color.

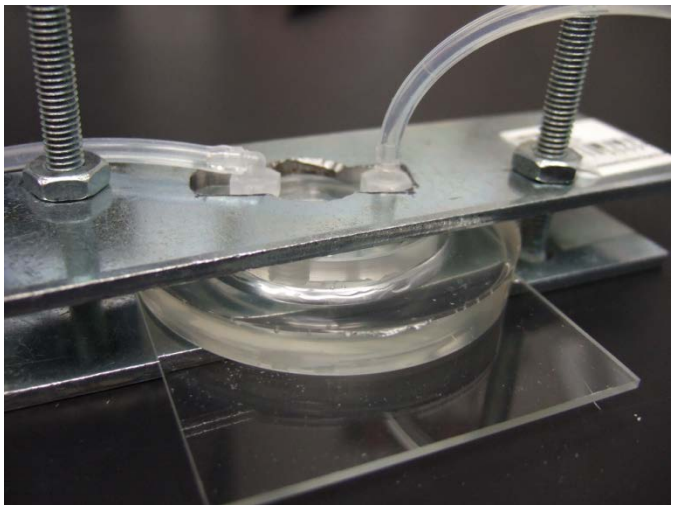

Figure 13: Modified flow chamber setup. Flow chamber is clamped with two metal Plates and screws in order to hold the flow deck on top of the hydrogel. Holes were drilled in the center of the metal plates for viewing under microscopes. A PMDS ring surrounds the flow deck to keep flow media from leaking, if any, into the microscope

2.8.1 Assumptions and Equations

To describe the fluid dynamics within the flow chamber, several assumptions were made. Figure 14 shows a schematic of the side view of a flow chamber with the Cartesian coordinate specified. The width and the length of the flow chamber is about 15 and 150 times larger than the height respectively, so it is assumed to be much larger than the height. Hence, end effects are neglected. The density of the flow media was assumed to be a constant and the flow was at steady state and steady flow. Steady flow assumption produces Equation (4), so flow in the *x*-direction was only considered. Together, these satisfy the equation of continuity (Equation (5)) and give Equation (6).

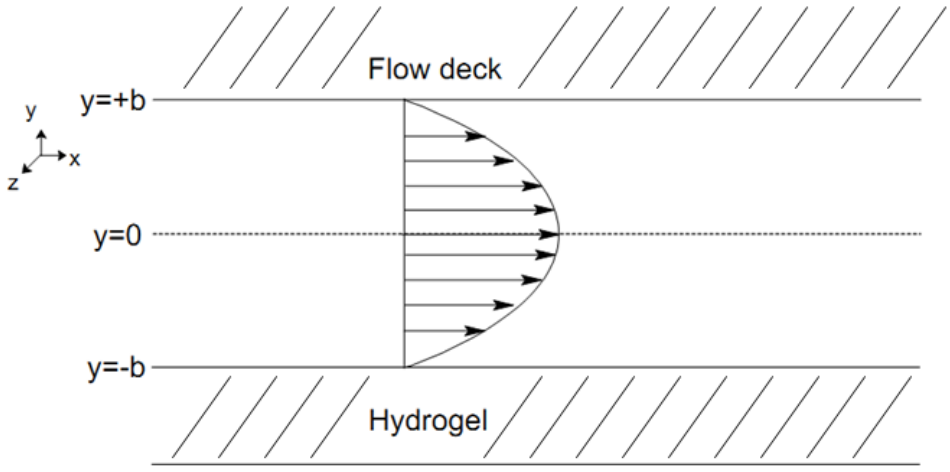

Figure 14: Qualitative velocity profile in parallel plate flow chamber. Using assumptions discussed in Section 2.8.1, parallel plate flow chamber shows a parabolic velocity profile.

$$v_y = 0,\ v_z = 0, v_x = v_x(y) \tag{4}$$

$$\frac{\partial \rho}{\partial t} + \frac{\partial}{\partial x}\rho v_x + \frac{\partial}{\partial y}\rho v_y + \frac{\partial}{\partial z}\rho v_z = 0 \tag{5}$$

$$\frac{\partial}{\partial x}\rho v_x = 0 \tag{6}$$

The walls of the flow chamber consist of the flow deck, the silicone gasket and the surface of the hydrogel. Rigid walls assumption is applied to assume the walls, which include the surface of the hydrogel, to be uninfluenced by the flow. The no-slip boundary assumption is also applied

$$y = \pm b, \qquad v_x = 0 \tag{7}$$

The flow chamber was placed horizontally, so gravitational effect can be neglected ($g_x = 0$). The flow medium was assumed incompressible and Newtonian. The

flow is laminar and Reynolds number is low. These satisfy the Navier-Stokes flow, so equation of motion in the *x*-direction (Equation (8)) simplifies to Equation (9).

$$\rho\left(\frac{\partial v_x}{\partial t}+v_x\frac{\partial v_x}{\partial x}+v_y\frac{\partial v_x}{\partial y}+v_z\frac{\partial v_x}{\partial z}\right) \tag{8}$$

$$=-\frac{\partial p}{\partial x}+\mu[\frac{\partial^2 v_x}{\partial x^2}+\frac{\partial^2 v_x}{\partial y^2}+\frac{\partial^2 v_x}{\partial z^2}]+\rho g_x$$

$$0=-\frac{\partial p}{\partial x}+\mu\frac{\partial^2 v_x}{\partial y^2} \tag{9}$$

Equation (9) can be written in terms of shear stress, τ_{yx}, and is shown in Equation (10). Taking the pressure of the inlet as P_0 and outlet as P_L, the difference between the inlet and outlet pressure is ΔP. The length of the flow chamber is L, so Equation (9) becomes Equation (10) and the shear stress τ_{yx} can be found. To solve Equation(10), the boundary condition shown in Equation (13) is able to obtain the constant C_1 to be 0.

$$\tau_{yx}=-\mu\frac{\partial v_x}{\partial y} \tag{10}$$

$$\frac{d\tau_{yx}}{dy}=\frac{\Delta P}{L} \tag{11}$$

$$\tau_{yx}=\frac{\Delta P}{L}y+C_1 \tag{12}$$

$$at\ y=0,\qquad \tau_{yx}=0,\qquad C_1=0 \tag{13}$$

To further solve for v_x, integration of Equation (12) gives Equation (14). Using the boundary conditions in Eqn.(7), C_2 is solved and v_x is shown in (16).

$$v_x=-\frac{\Delta P}{2\mu L}y^2+C_2 \tag{14}$$

$$0=-\frac{\Delta P}{2\mu L}b^2+C_2, C_2=-\frac{\Delta P}{2\mu L}b^2 \tag{15}$$

$$v_z = \frac{\Delta P}{2\mu L}(b^2 - y^2) \tag{16}$$

Besides the velocity at *x*, the average fluid velocity can also be found by integrating Equation (16) and gives Equation (17).

$$\langle v_x \rangle = \frac{1}{2b}\int_{-b}^{+b} \frac{\Delta P}{2\mu L}(b^2 - y^2)dy \tag{17}$$

$$= \frac{\Delta P}{2\mu L}(b^2 y - \frac{1}{3}y^3)|_{-b}^{+b} \tag{18}$$

$$= \frac{\Delta P b^2}{2\mu L} \tag{19}$$

For parallel plate flow chamber, the shear rate, $\dot{\gamma}$, is shown in Equation (20), where *Q* is the volumetric flow rate (mL/s), w is the width of the chamber and *h* is the height of the chamber [81]. To evaluate shear stress, τ_{yx}, Equation (21) was used.

$$\dot{\gamma} = \frac{6Q}{wh^2} \tag{20}$$

$$\tau_{yx} = \mu\dot{\gamma} \tag{21}$$

Due to the fact that there was a lack of ability to measure pressure drop, ΔP, average fluid velocity was estimated with Equation (22). Using the estimated average fluid velocity, ΔP was estimated and v_x was determined.

$$v_{avg} = \frac{Q}{w2b} \tag{22}$$

2.9 ECFCs Rolling

Cell rolling is a phenomenon that has been historically observed in the recruitment of leukocyte during inflammation. When a leukocyte comes in contact with the endothelium, the surface receptors on the leukocyte interact adhesively with the

ligands present on the endothelium. However, this adhesion is transient due to the shear force by blood flow. This force causes the leukocyte to roll along with the flow stream until the adhesiveness of leukocyte on endothelium is strong enough to withstand the shear [44]. The strength of the adhesion depends on the number and types of bonds are formed between the leukocyte and the endothelium. Cell rolling is the result of a balanced bond formation and breakage, and it seems to be a necessary step before leukocyte is firmly adhered to the endothelium. Cell rolling velocity can be used to characterize cell rolling [60] and it is determined as the mean of instantaneous velocity during rolling.

As mentioned in Section 2.3.1, leukocytes include myeloid cells and lymphoid cells. Although research is still ongoing, EPCs are thought to be derived from leukocytes, specifically from myeloid cells, and perhaps are one kind of monocyte. Although EPC rolling has not been widely investigated, the EPC rolling phenomenon has been observed. An *in vitro* study by Angelos *et al.* has shown that umbilical cord blood derived EPCs (CB-EPCs) roll on fibronectin and bovine serum albumin (BSA) coated surfaces. An *in vivo* study has provided evidence of embryonic EPC (eEPC) moves along the vessel wall within seconds [82]. Figure 15 shows a sequential intravital microscopic images of two labeled eEPCs, 1 and 2. eEPC 1 was firmly captured to the vessel wall under flow and eEPC 2 was moving along the vessel wall from Figure 15B to Figure 15D in 4 s. Figure 15E shows that eEPC 2 was sheared away from the vessel wall at the end of the 4 s. Therefore, EPC rolling was observed in both *in vivo* and *in vitro*.

2.9.1 EPC Rolling on Hydrogel

As seen in the *in vivo* and *in vitro* examples mentioned above, EPCs possess the ability to roll on either endothelium or ECM proteins. To develop a biomaterial that is suitable for supporting EPCs, the investigation of ECFC rolling provides strong insight in understanding the interaction between ligands and EPC surface receptors. As mentioned in Section 2.4, PEG hydrogels have great potential in serving as vascular grafts coatings, especially with respect to their ability to limit protein absorption and their flexibility which is similar to natural tissue. Using the grafting technique, peptides of interest can be immobilized on PEG hydrogels to evaluate the potential of these peptides-grafted hydrogels as biomaterial for ECFCs. Therefore, characterizing rolling velocity of EPC on a hydrogel material is essential. To my knowledge, all studies investigating in EPC rolling have been limited to the use of on ECM proteins which bind a wide range of cell surface receptors. This study is robust and unique in that it investigates EPC rolling on a biomaterial surface and examines individual receptor interactions.

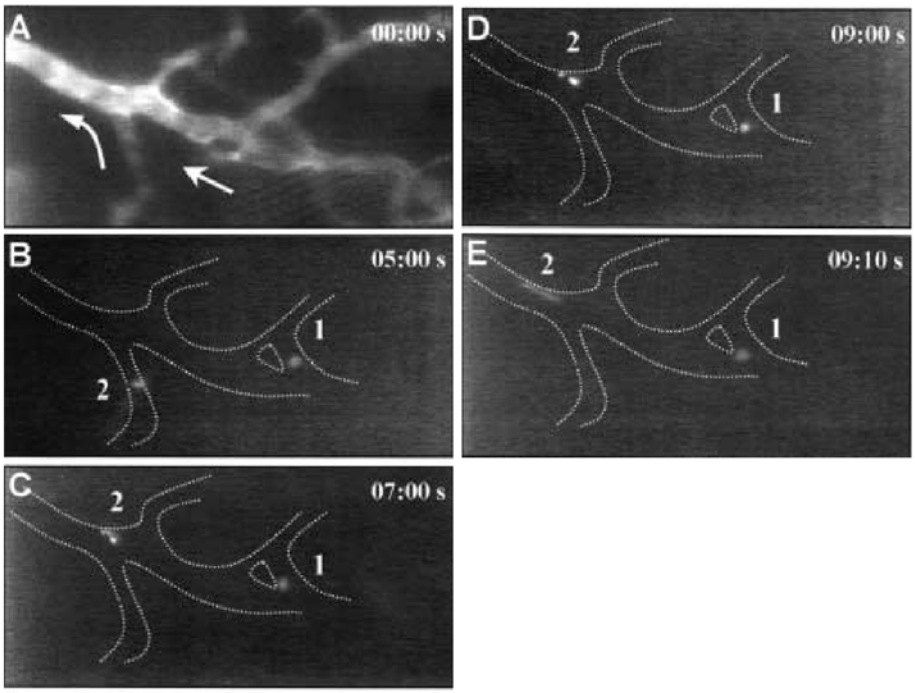

Figure 15: Sequential intravital microscopic images of two labeled eEPCs. A) Arrows indicate the direction of blood flow in the tumor blood vessel of the skinfold chamber of nude mice. B) eEPC 1 and 2 were fluorescently labeled and eEPC 1 was captured at bifurcation while eEPC 2 was transiently adhering onto the tumor endothelium. C) eEPC 1 did not moved and was shown to be firmly adhered whereas eEPC 2 reached another location of the endothelium at 2 seconds later. D) Both eEPC 1 and 2 continued to be captured at the same location. E) eEPC 1 remained adhered and eEPC 2 was washed away by the blood flow. Reprinted from Vajkoczy et al., 2003 (copyrighted). Originally published in *The Journal of Experimental Medicine*. Vol:197–12.

2.9.2 Rolling Cell Tracking Using ImageJ and MATLAB

Cell tracking and analysis on rolling cells under flow has been traditionally labor intensive and inefficient. To obtain the instantaneous cell velocity, one has to first manually identify the position of each cell on a frame-by-frame basis in the video recording [2]. Then the displacement for each cell can be obtained and used in calculating cell velocity. However, as the number of cells increases, the tracking time also increases

tremendously. In addition, as the speed of the camera, in other words frame rate, increases, the amount of data and therefore the time needed to analyze the data becomes unmanageable. With the development of computer program algorithms for cell identification, position of each cells can be found automatically. Besides eliminating the need for tedious manual cell tracking, computer program algorithms also avoid bias that can be introduced by investigator [15,55,76]. Therefore, using computer program algorithms for cell tracking provides advantages in repeatability and high throughput.

There are some additional problems in cell tracking and analysis that cannot be solved easily with computer program algorithms. For example, there are two critical problems that occur in tracking ECFC rolling. The first one is long computation time due to the complexity in tracking algorithm. In my preliminary testing, I tested a shape-based centroid tracking algorithm for MATLAB that was developed by Schmidt *et al.*; this research group is well known for their knowledge in cell tracking under flow. Their system is fully automatic and highly accurate, but requires excessive processing time due to steps such as deconvolution, cell internal blurring, gradient computation, and object detection [69].According to my testing, even 10 hours of processing was insufficient to analyze a two minute 500 x 240 pixel video recorded at 70 fps using a computer with Intel Core i7 at 1.7s GHz and 6GB RAM. Besides processing time, incompatibility between video codec and operating systems caused issues in loading the video files. Although this codec issue can be overcome by converting the video into a compatible format, the video conversion takes almost an hour to complete. The second problem is that the tracking algorithm is frequently confused by cells that come close in proximity to each other or come in contact with each other. Hence, the position of each cell cannot be

identified properly which leads to erroneous outcomes for cell rolling velocity. Other non-MATLAB based cell tracking software also has the exact same problem. Software that I have tested includes Nikon NIS-Elements, CellTrack, and Tracker. Therefore, this motivated me to create an alternative approach that is faster and more efficient.

The ECFC rolling tracking system in this study was developed to decrease the computation time and eliminate the issue of incorrect cell tracking due to cells that come into close proximity or contact with each other. Using this tracking system, the average time needed to track a 2 min cell rolling video at 70 fps is less than 20 min, which is a very significant decrease, and the issue of excluding interacting cells from the tracking data was also solved. The approach developed in this study for tracking rolling ECFCs under flow is divided into two main processes. The first process uses ImageJ, a public domain imaging software by NIH, to identify the position of each cell on each frame and the second process takes all the position data and matches them for each cell using MATLAB. Finally, the tracked data are analyzed using VBA in Excel as shown in Figure 16. The advantage of using ImageJ for identifying cell position is that ImageJ has preset thresholding methods that can efficiently and rapidly identify the edge of each cell. Each of these preset methods determine an optimal threshold level using their specific thresholding method. ImageJ also allows the user to manually setting the threshold when these methods cannot provide the best result. In most cases, these thresholding methods are able to identify the edge of each cell. The thresholding methods that were used frequently in this study were Intermodes, IsoData, and MaxEntropy. (The details of each method will not be discussed here since this is not the major focus of the study, but the

details can be found on the ImageJ official site [17].) The steps developed in this study to identify cell position are as follows:

1. Convert each frame into 8-bit (Figure 17a)
2. Apply thresholds to each frame and convert them into black and white images so that each cell appears to be a white ring object with black background (Figure 17b)
3. Fill in the hole of each white ring to obtain solid white objects(Figure 17c)
4. Find the position of each cell (solid white objects) with respect to the preset parameters including size and roundness (Figure 17d)

To avoid confusion during tracking caused by cells that come in contact, only single cell rolling is considered. For cells that come in contact, together they have a larger area and a much lower roundness when compared to single cells, so identification parameters, such as the acceptable range for cell area and roundness, were set in ImageJ to prevent tracking of these cells. The identification parameters also served to exclude tracking of undesired objects including small debris and big cell clumps that occasionally appeared in the flow media. To make sure only single cells were tracked, objects appearing along the edge of the field of view are also excluded. Details for each identified cell, including *x* and *y* coordinates, cell area, cell roundness, and frame number, are output into an Excel file for matching using MATLAB. A custom ImageJ macro was written to run all these steps for each video file.

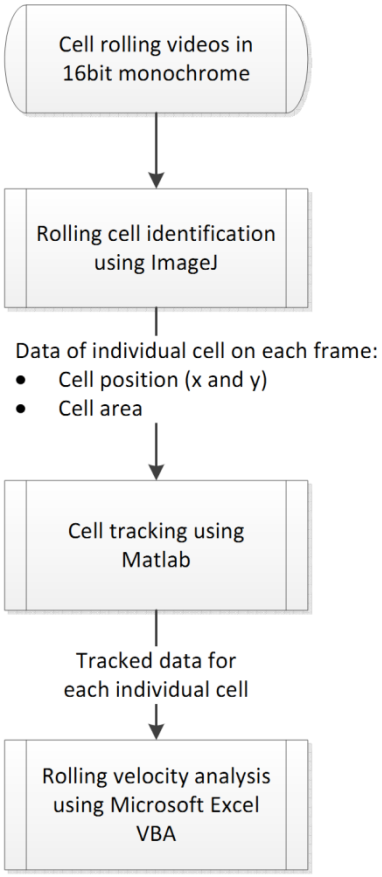

Figure 16: Work flow of cell tracking using ImageJ and MATLAB.

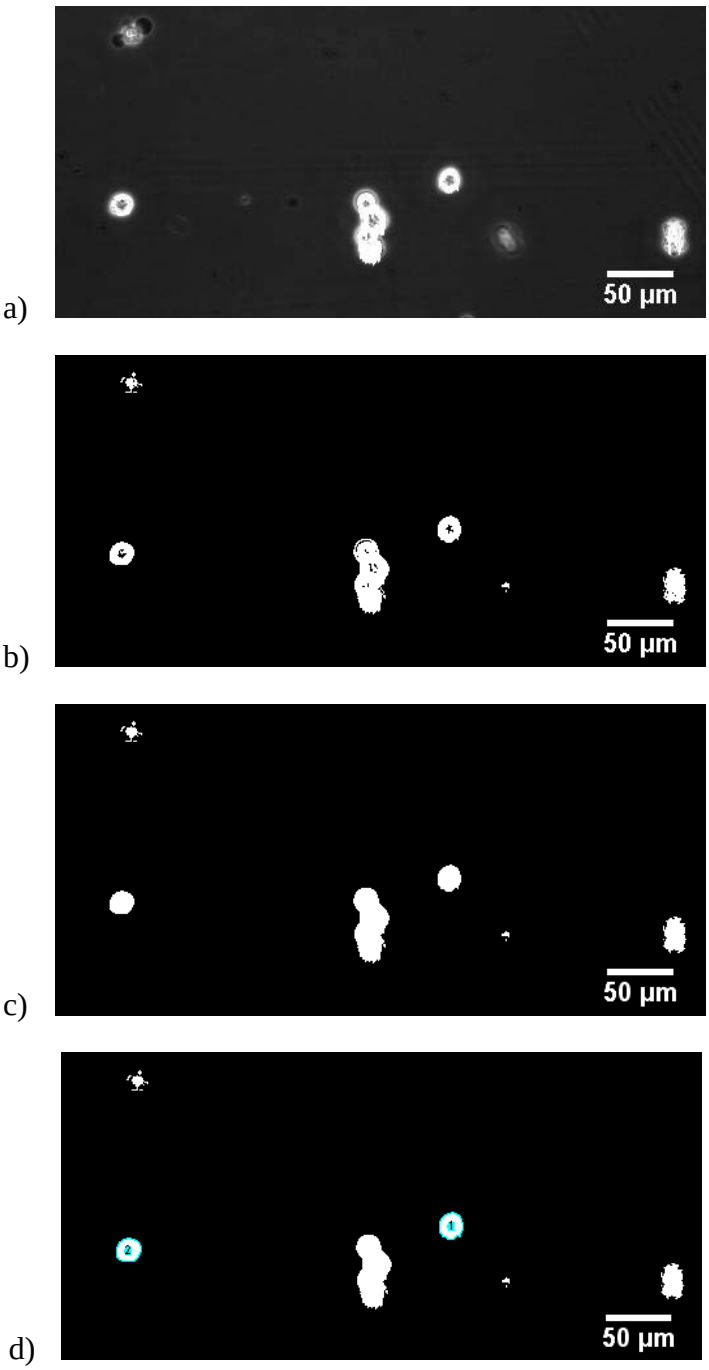

Figure 17: Representative images of rolling ECFCs identification process by ImageJ. a) Image converted to 8-bit from 16-bit. b) ImageJ filter was applied to produce black and white image. c) Internal holes were filled. d) Representative of tracked image showing the tracked ECFCs with label.

After using ImageJ to identify the positions of ECFCs on each frame, the data are imported to MATLAB for matching. The matching process correlates the data for each individual cell on a given frame with the data for each cell on the next frame. Using this process, the positions of each individual cell are output in sequential order. A cell pool was first setup by including all cells in the first frame for matching. Then, all cells appeared in the next frame were matched to each cell in the cell pool according to three major requirements. First, the *y* position of a cell in a new frame must be equal or less than 8 μm comparing to the cell for matching in the cell pool. Since the cells are flowing horizontally across the flow chamber, the cell cannot be the same cell if there is a substantial difference in the *y* coordinate in consecutive frames. Most ECFCs have an average diameter of 15 to 20 μm in suspension, so 8 μm, which is about half of the ECFC diameter, was determined to be sufficient for *y* coordinate restriction condition. Second, the difference of area of a cell must be equal or less than 30% between the frames. A change in 30% of cell area corresponds to a change in 15% in cell diameter. Due to being out of focus, cells on a higher focal plane appear to be larger than the cells in focus on the bottom of the flow chamber. Therefore, this restriction on change in cell area was implemented. Third, the displacement of a given cell must not be greater than the distance physically possible for it to have moved at the fluid flow velocity being tested. A cutoff on displacement distance between frames was therefore used to prevent potentially mismatched cells. This distant is dependent on both the fluid flow velocity at a one cell diameter away from the wall, which changes with the shear rate being tested, and the rate of data acquisition, i.e. frames per second. In the process of matching, an upper limit on *x* displacement, Δx in Equation (23), was used. To determine Δx, an *x* displacement

parameter, $x_{shear\ rate}$, and a scaling factor, $\frac{70\ \text{fps}}{\text{current frame rate}}$ were implemented, as shown in Equation (23). For a cell to be matched between sequential frames, this *x* displacement must be within the range that is physically possible. At a certain frame rate, the *x* displacement parameter of a cell depends on the shear rate of the fluid in the flow chamber. For example, the fluid flow velocity at a distance of 20 μm away from the bottom plate is estimated to be 730 μm/s at 40 s^{-1}, so the *x* displacement of a cell must be equal or less than 10.4 μm at 70 fps. Through trial-and-error, a *x* displacement parameter of 10 μm was found to effectively prevent incorrect cell matching for shear rates of 20 s^{-1} and 40 s^{-1}, and 20 μm for shear rates of 80 s^{-1} and 120 s^{-1} for videos recorded at 70 fps. Important to consider is that the frame rate of the high speed camera fluctuates slightly over the course of experiments, because of the increase in the camera temperature. Therefore, the scaling factor, as shown in Equation (23) was used to account for differences in video frame rates. Due to the instances where cells were not identified by ImageJ because of overlapping cells on a different focal plane, this matching process is allowed for cells that are up to 7 frames apart. Thus, cells that are not matched for 7 frames or more are removed from the cell pool. After data for each cell is matched, displacement distance and instantaneous velocity are calculated. This matching process is looped until the last frame of each video; the matching logic is shown a flow chart in Figure 18. After the matching by MATLAB, important data including average rolling velocity and percentage of rolling frame for each cell can be obtained for analysis.

$$\Delta x = x_{shear\ rate} \times \frac{70\ fps}{current\ frame\ rate} \tag{23}$$

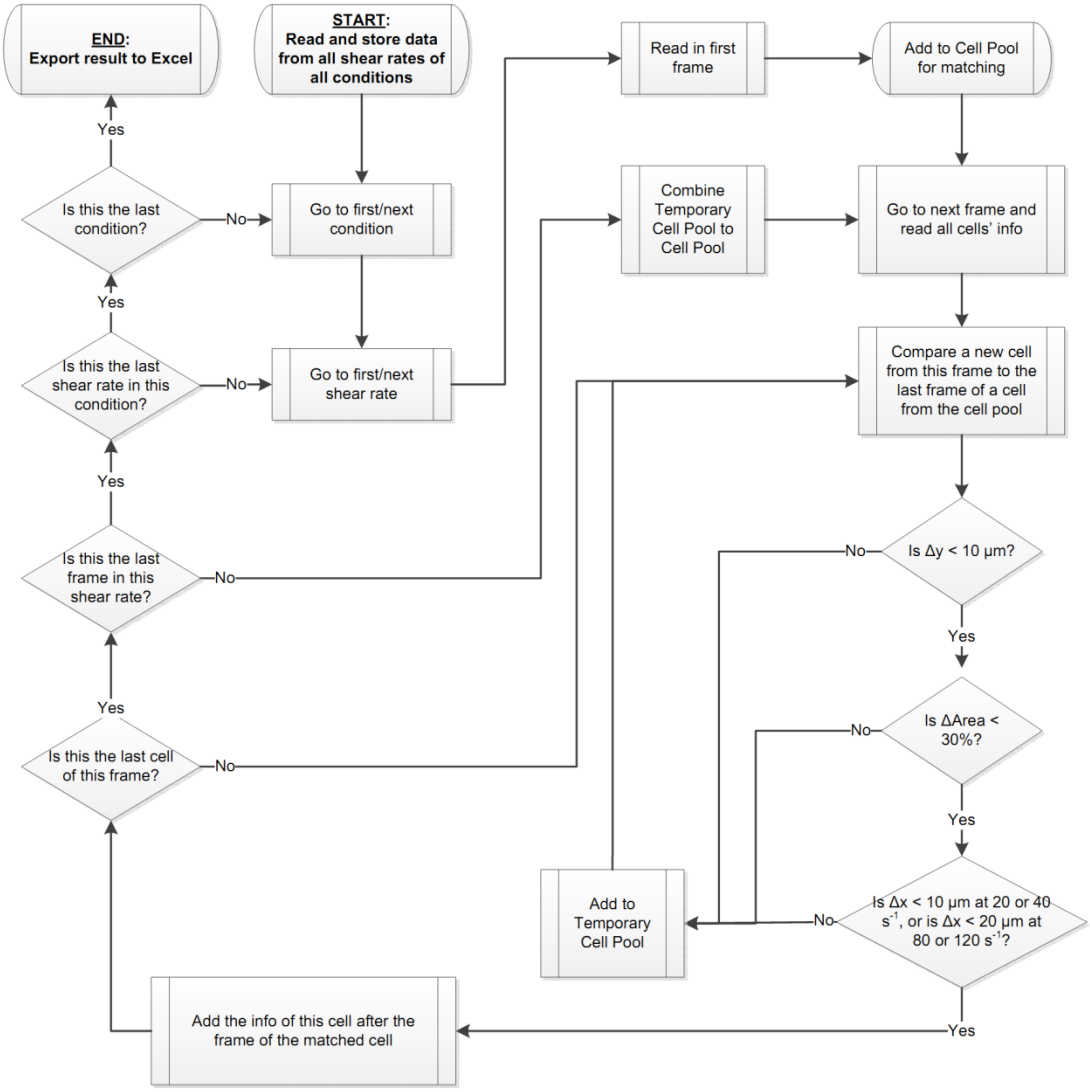

Figure 18: Flow chart of the matching process using MATLAB. Multiple nested loops were used to run through all conditions, shear rates, frames, and cells on each frame. Three major matching parameters were Δ*y*, ΔArea, and Δ*x*.

2.10 ECFCs Migration

Endothelial migration plays an important role in the closure of denuded area in small vessel injuries [93]. There are three major mechanisms involved in cell migration: chemotaxis, haptotaxis, and mechanotaxis. In chemotaxis, ECs migrate in the direction of a gradient of soluble chemoattractant. The major promoters of EC chemotaxis are

vascular endothelial growth factor (VEGF), basic fibroblast growth factor (bFGF) and angiopoietins. These growth factors bind to EC receptors and stimulate multiple downstream pathways that regulate cell migration [43]. Haptotaxis corresponds to the directional migration due to a gradient of immobilized ligands. Usually, ECM proteins represent the ligands. For example, fibronectin has been show to enhanced VEGF-mediated CD34+ cell migration [89]. In my study, the peptides grafted onto the hydrogel surface are the immobilized ligands for ECFCs migration. Lastly, shear stress is the major type of mechanotaxis for ECs. Shear stress stimulates signaling pathways that are responsible for actin cytoskeleton remodeling. The cytoskeleton is given polarity when it is exposed to shear; this can be illustrated *in vitro* when ECs align themselves parallel to the direction of fluid flow.

2.10.1 General EC Migration

During EC migration, the actin cytoskeleton possesses polarity and migrates according to a gradient. There is a constant remodeling of actin cytoskeleton into filopodia, lamellipodia, and stress fibers. Figure 19 shows the sequential steps during migration. First, filopodia on EC sense the motile stimuli. Second, cellular extension occurs through the protrusion of lamellipodia that serves as the leading edge of EC. Then the protrusions form attachments with ECM at focal adhesions. Finally, the cell body is contracted by stress fibers and the rear edge of EC releases. This cycle is repeated until the end of migration.

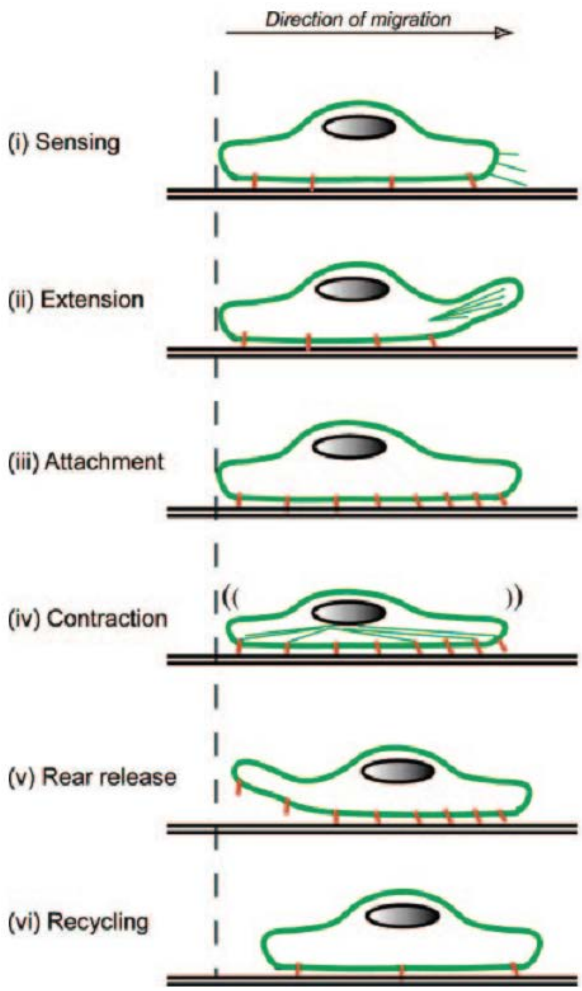

Figure 19: Sequential events of endothelial cell migration. i) Sending of attractant with filopodia. ii) The lamellipodia of the leading edge extends forward. iii) The protusion forms attachment with the ECM. iv) Stress fibers causing contraction. v) Contraction cause the rear to release and move forward. vi) Recyling to the sensing step. Reprinted with permission from Ref 43.

Two types of endothelial cell migration assays are commonly seen in the literature: wound healing and Boyden chamber assays. In wound healing assays, a wound is created on a confluent monolayer of ECs by scratching the surface with a solid object. Endothelial cells tend to migrate into the "wounded" area to reform the confluent layer and the migration speed is observed. In Boyden chamber assays, the migration of ECs

through a porous membrane from one chamber to the other is observed. The top chamber is the EC seeding chamber and the bottom chamber contains the chemoattractant which attracts the ECs. This assay provides a quantitative means to evaluate the effect of the chemoattractant by measuring the number of migrated cells.

2.10.2 Migration of ECFCs on Hydrogel Surface

To study the potential of using hydrogels to support ECFC endothelialization, a custom migration assay was designed. Similar to the wound healing assay, this custom assay allows ECFCs to migrate on the flat surface of hydrogel. However, a confluent layer of ECFCs was allowed to migrate outward from a boundary in order to evaluate the ability of ECFCs to endothelialize into an extensive region of the hydrogel surface, instead of evaluating the time and ability for ECs to reform the endothelium across a relatively narrow wounded site in wound healing assay. In this custom migration assay, a PDMS seeding mold was placed on top of the hydrogel with clamps. The seeding mold has a rectangular seeding chamber that allows ECFCs to be seeded as shown in Figure 20. After ECFCs were adhered and become confluent, the mold was removed. ECFCs formed a distinct boundary as shown in Figure 21 that served as the starting point and ECFCs were allowed to migrate for 72 hours. This custom assay provided the advantage in obtaining an accurate migration distance, which has been shown to be a challenge on hydrogels.

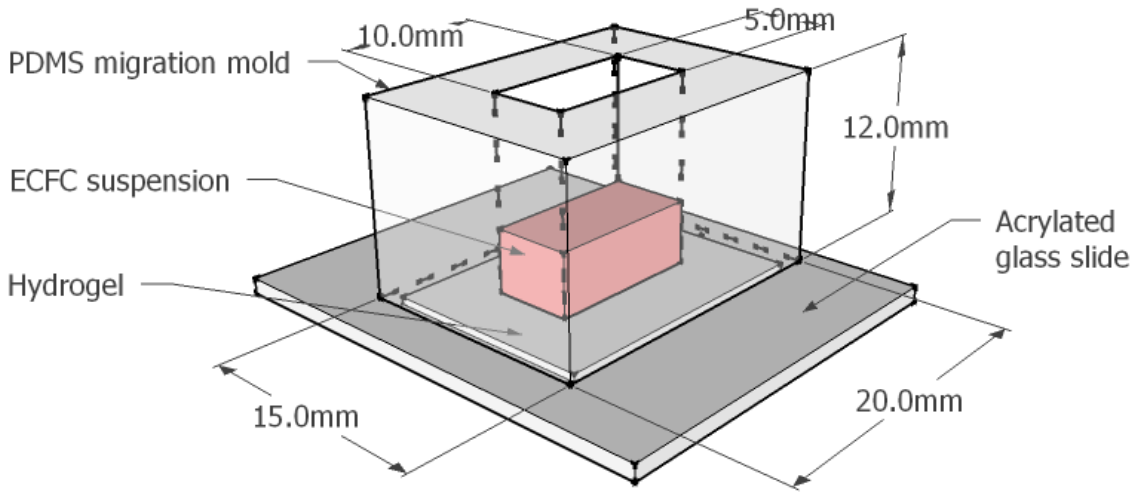

Figure 20: A sketch with the dimensions of a migration PDMS seeding mold. The seeding mold is placed on top of a peptide-grafted hydrogel that was formed on an acrylated glass slide to keep the hydrogel immobilized. ECFCs were able to be seeded on the seeding area on the surface of a hydrogel. Sketch was produced by using Google Sketch Up.

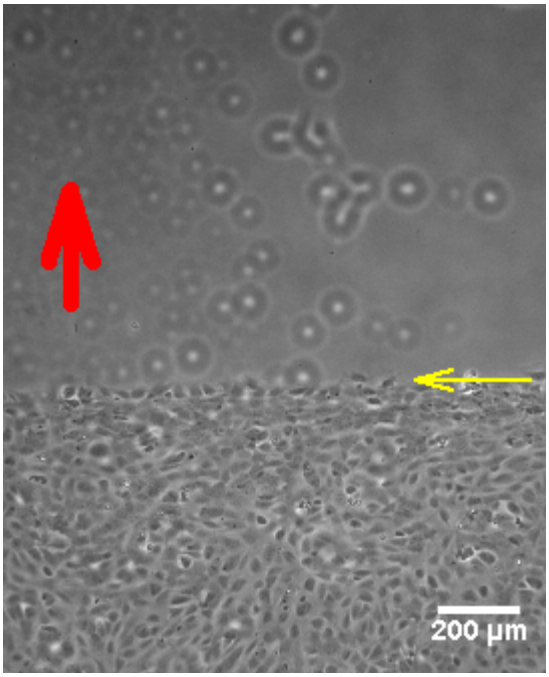

Figure 21: The beginning of ECFC migration. After 24 hours of seeding, the PDMS seeding mold was removed and the ECFCs formed a straight boundary, indicated by the yellow arrow, to serve as the starting point for migration. Red arrow indicates the direction of ECFCs migration.

3. EXPERIMENTAL DETAILS

3.1 ECFCs Culture

Human umbilical cord blood derived ECFCs (Poietics Human Endothelial Colony Forming Cells, Lonza) was cultured in either T-25 (Cellstar) or T-75 (BD) flasks with 0.2 mL/cm^2 of ECFC media (Lonza) within a biosafety cabinet (Labconco) to maintain sterility. Flasks were coated with collagen (BD) in a concentration of 50 μg/mL in 0.02 N acetic acid (Pharmco-aaper) at least 1 hour prior using. ECFCs were incubated in an incubator (Napco 8000 WJ, ThermoFisher Scientific, Waltham, MA) controlled at 37°C and 5% CO_2 and partial media change was performed every other day until it reached 80-90% confluent for subculture. Subculture was done by first rinsing with warm PBS (Lonza), which was prepared by diluting from 10X into 1X using autoclaved 18.2 MΩ de-ionized (ultrapure) water following filter sterilization with 0.22μm filter (Millipore). Then ECFCs were incubated with 0.025% trypsin (Lonza) for 0.05 mL/cm^2 at 37°C for 1.5 min. When most ECFCs in the culture flask were rounded, the cells were loosened off the flask surface by gently tapping the side of the flask. Trypsin was neutralized by the addition of ECFC media with twice the amount of trypsin, followed by centrifugation (Eppendorf) at 200 g for 5 min. Cells were resuspended in ECFC media and subcultured at a ratio of 1:3 before incubation. Only passage 8 to 16 of ECFCs were used for experiment.

3.2 Photoinitiator Cell Viability

Photoinitiators, including I-2959, DMPA, and I-184, were dissolved into concentrations of 0.03, 0.05, and 0.1 g/mL in 70% ethanol. Eosin Y was dissolved into concentrations of 0.003, 0.007, and 0.014 g/mL in 70% ethanol. ECFCs were suspended

in media and diluted to 20,000 cells/mL. 500 μL of ECFC suspension was added into each well of 48-well plates. The prepared photoinitiators were added to the ECFC suspension at a concentration of 5 μL/well. Control was set up with only the addition of 70% ethanol but not any photoinitiators. After 1 hour of incubation at 37°C, ECFCs that were incubated with I-2959, DMPA, I-184, and control were exposed to UV light at 365 nm for 5 min while ECFCs that were incubated with eosin Y and control without eosin Y were exposed to visible light for 5 min. Another control to study the effect of UV or visible light exposure was setup by covering the plates with foil to keep the plates from exposing to UV or visible light.

After a 48-hour incubation, ECFCs were assayed for viability using WST-1 metabolic indicator (Fisher). ECFCs were rinsed with 250 μL PBS and 500 μL of ECFC media was added. 50 μL of WST-1 was added per well and incubated at 37°C for 2 hours. Cell viability was quantified by measuring the absorbance at 420 nm with a Biotek Synergy HT microplate reader. The effect of background was accounted by subtracting the average empty well reading from all values. Sample values were scaled linearly from 0 to 1. Wells with media only had a value of 0 while wells with the addition of 70% ethanol to ECFCs had a value of 1.

3.3 Hydrogel Formation

3.3.1 PEG Acrylation

Poly(ethylene glycol) (PEG, 6kDa; Sigma) was first lyophilized at -50°C and 0.03 mbar overnight before reaction. Each batch of polyethylene glycol diacrylate (PEGDA) was prepared by reacting 24 g of the lyophilized PEG with 0.016 mol of

acryloyl chloride (Alfa Aesar) and 0.008 mol of triethyl amine (TEA, Sigma) in up to 40 mL of anhydrous dichloromethane (DCM, Acros) under argon (Airgas) for at least 12 hr or overnight. Two moles of 1.5 M K_2CO_3 (Fisher) were added per initial mole of acryloyl chloride with vigorous shaking and the mixture was allowed to separate for at least 3 days. The organic phase was collected and anhydrous $MgSO_4$ (Fisher) was added to remove the trace amount of aqueous solution. Vacuum filtration was performed to filter out the $MgSO_4$ in the solution. The PEGDA in the organic solution was precipitated by adding into 1.6 L of cold ethyl ether and stirred for 10 min to move TEA into the organic solution. Then, PEGDA was collected by vacuum filtration and air dried thoroughly to allow most of the ethyl ether (EMD) to evaporate. The PEGDA was further dried by lyophilization or dried under vacuum. PEGDA was then aliquoted and stored under argon at -20°C. The extent of acrylation was estimated by NMR analysis.

3.3.2 NMR Analysis

After each batch of PEG-DA was prepared, the acrylation percentage was estimated by NMR analysis to characterize the yield of the acrylation process. Sample of PEG-DA was dissolved in 50 mg per 0.75 mL in deuterium oxide (D_2O, Acros) and injected into NMR tube (VWR) that was pre-cleaned with acetone (Macron). Analysis was done by Bruker 400 MHz NMR. Parameters in refining the analysis were used according to the suggested equipment protocol. By setting the D_2O peak at 4.8 ppm, peaks for acrylate single protons were found at around 6.00, 6.20, and 6.45 ppm while the peak representing PEG was found at 3.70 ppm. Integrated intensity peaks were found and used in estimating acrylation percentage and were shown in sample calculations shown in Appendix A.

3.3.3 Peptide Synthesis

An automated peptide synthesizer APEX396 SC (Aapptec, Louisville, KY) was used to synthesize the peptides applying solid phase chemistry at room temperature with continuous nitrogen supply that served as an inert atmosphere. Fmoc-Gly-Wang resin and amino acids were first thawed to reach the room temperature before measuring the needed quantity. 600 mg of resin was placed in each chemically resistant Teflon reactor block. Each amino acid solution was prepared in 0.4 M in reagent bottles. After synthesis was completed, peptides were cleaved off from resin in the cleavage block. The cleavage solution was prepared by mixing 95% TFA, 2.5% TIPS, 2.5% ultrapure DI water by volume and used at 10 mL/g of resin. Peptides were collected in the glass collection vessels and poured into centrifuge tubes for air drying. After most of the cleavage solution was evaporated, the peptides were washed three times with cold ether under centrifugation at 4,000X g for 2 min each to remove the left over TFA. After the ether was discarding, the peptides were air dried and prepared for lyophilization. Peptides were then aliquoted into brown glass vials and stored under argon at -80°C.

3.3.4 Characterization of Peptides by Mass spectrometry

Peptide synthesis was confirmed by mass spectrometry. A tiny amount of peptide (<1 mg) was dissolved in 10% acetonitrile and 0.1% formic acid injection solution. Result mass was obtained using Q-TOF Premier (Waters, Milford, MA) and shown in Appendix B.

3.3.5 PDMS Molding

PDMS spacers and seeding molds were created with Sylgard 184 silicone elastomer kit (Dow Corning) in aiding migration study. Base and curing agent were

measured in a 10:1 weight ratio on a disposable weighing dish and mixed vigorously for 3 min. De-gassing of the mixture was done by pulling vacuum in a dessicator. The mixture was then poured into either glass or polystyrene molds, and baked in an oven at 75°C for 1.5 hours. After curing, desired shape was removed from the PDMS using a punch or a blade. Then, PDMS molds were cleaned by sonication in 70% ethanol for 1 hour to remove uncured molecules. After each use, PDMS molds were cleaned and stored in 70% ethanol.

3.3.6 Hydrogel Crosslinking

Hydrogel precursor solution was prepared and crosslinked in biosafety cabinet to keep the hydrogel sterile. First, precursor solution was prepared by adding sterilized PBS to PEGDA to a concentration of 200 mg/mL. Since clumps of PEGDA were present after adding PBS, PEGDA is dissolved by first vortexing for 15 s and then a short centrifugation for 10 s. The dissolved PEGDA solution was filter sterilized by passing through a syringe filter (Millipore) having a pore size of 0.22 μm. Photoinitiator was prepared by dissolving DMPA (Acros) in N-vinylpyrrolidinone (Aldrich) at a concentration of 300 mg/mL. The photoinitiator was added to PEGDA solution at 10 μL/mL, where vortexing and centrifugation were also performed, to form the hydrogel precursor solution. The precursor solution was used immediately after it was prepared.

Hydrogel precursor solution was crosslinked with the use of a hydrogel crosslinking mold that consists of three components, including a 0.5 mm thick PDMS spacer, two pieces of rectangular microscope glass slides, and binder clips. Before use, the PDMS spacer was dried completely with nitrogen gun while the glass slides were soaked in a base bath prepared with 1M potassium hydroxide (KOH) (Fisher) in ethanol

for at least 3 hours and then rinsed with DI water following air drying. All components were setup together and shown in Figure 22.

a)

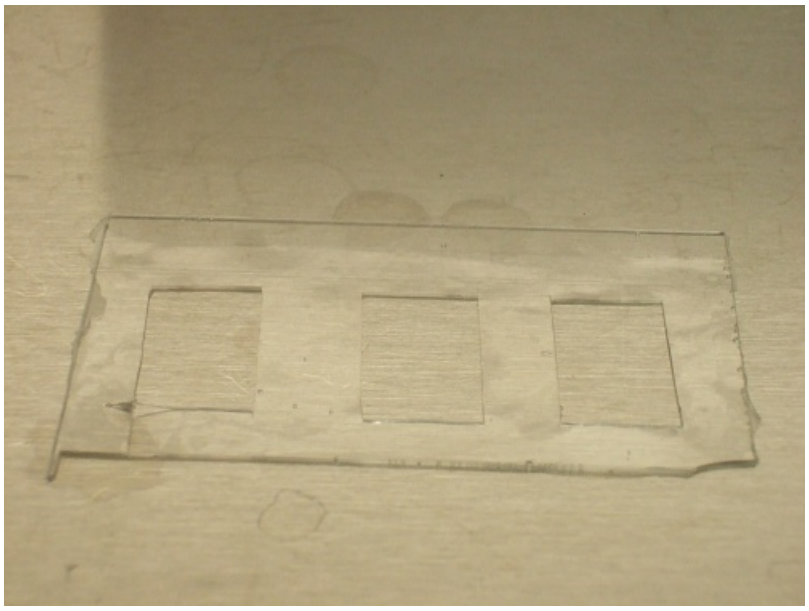

b)

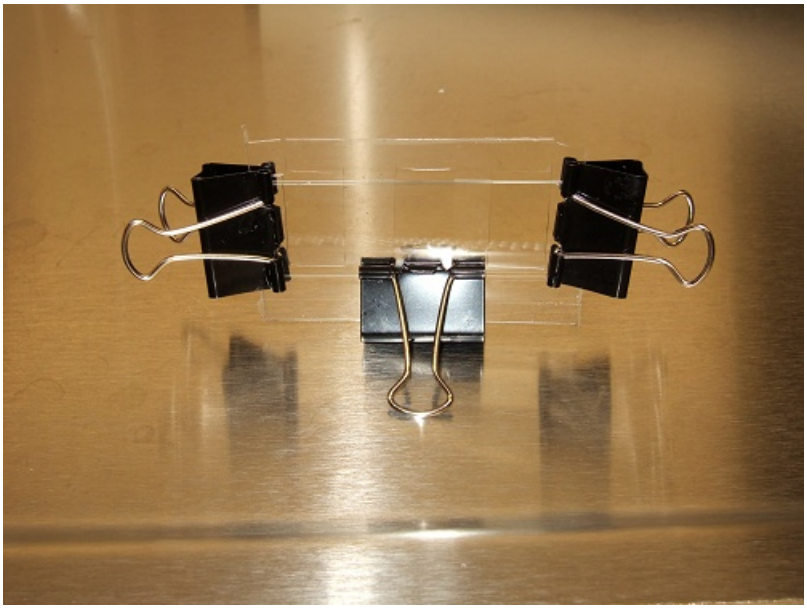

Figure 22: Hydrogel crosslinking molds. a) 0.5 mm thick PDMS spacer for crosslinking hydrogel. b) PDMS spacer was placed in between two pieces of glass slides and binder clips were used to hold them together. Polymer precursor solution was injected into the gap created by the spacer for crosslinking.

Hydrogel precursor solution was injected into the mold and placed horizontally under a pre-warmed 365 nm UV lamp (Cole-Parmer) with an average intensity of 3 mW/cm^2 at a distance of 2.5 cm for 5 min as shown in Figure 23. After the PEG hydrogel was formed, it was rinsed with sterile PBS and briefly dried using a nitrogen gun before peptide grafting. For use as a control, PEG hydrogel was placed in sterile PBS to swell before use.

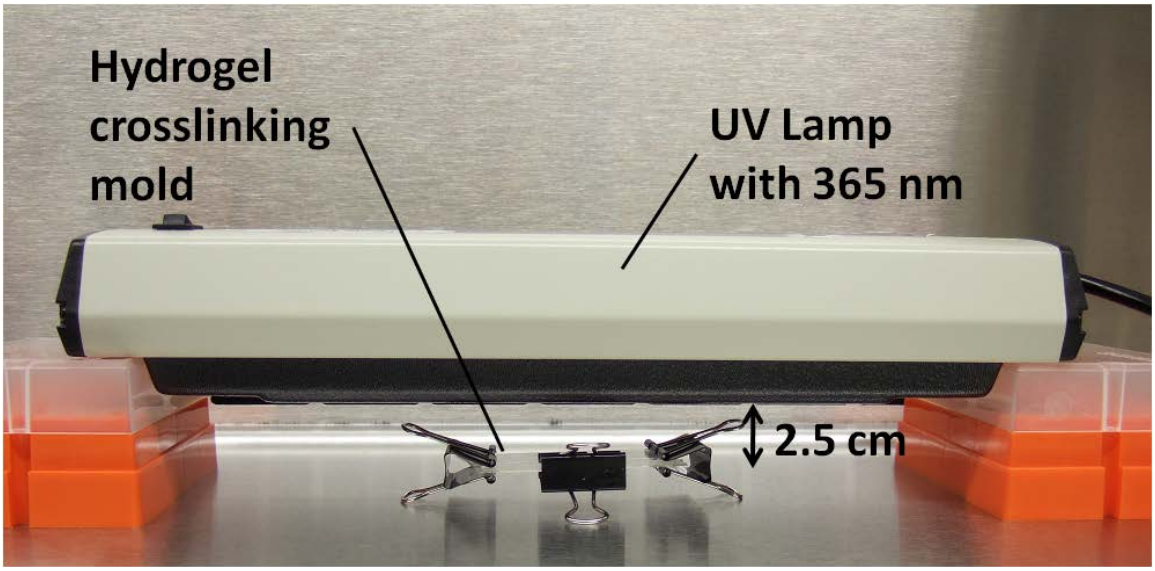

Figure 23: Hydrogel crosslinking mold was placed at a distance of 2.5 cm away under a UV lamp.

3.3.7 Hydrogel Grafting with Peptides

Peptides, either synthesized or purchased, were conjugated to acryloyl-PEG-succinimidly valerate (acryloyl-PEG-SVA, 3400Da; Laysan Bio) first before grafting on PEGDA hydrogel. Acryloyl-PEG-SVA was dissolved in 1 mL of 50 mm sodium bicarbonate buffer (pH 8.5) for every 10 mg of peptide used. For hydrophilic peptides, they were dissolved into a concentration of 0.04 mg/μL in the sodium bicarbonate buffer and the pH was adjusted to 8.5, if necessary, using HCl (Acros) or NaOH (Fisher). For hydrophobic peptides, they were dissolved in 2 M excess N,N-diisopropylethylamine

(DIPEA, Sigma-Aldrich) in DMSO. The peptide solution was added dropwise to the acryloyl-PEG-SVA solution with mild vortexing. The mixture was allowed to react on an orbital shaker within a foil-wrap for 4 hours at room temperature. The product acryloyl-PEG-peptide was dialyzed using a dialysis membrane with molecular weight cutoff (MWCO) of 500-1,000 (SpectrumLabs) and lyophilized for storage under argon at -80°C in a brown glass vial.

The acryloyl-PEG-peptide was dissolved in sterile PBS into the concentration needed and photoinitiator was added in 10 μL/mL in a foil-wrapped microcentrifuge tube, where vortexing and centrifugation were also performed. This peptide grafting solution was used following the crosslinking of PEG hydrogel. After the PEG hydrogel was formed, the top plate of the mold was removed, the hydrogel was rinsed with sterile PBS and briefly dried with a stream of nitrogen to remove excess PBS on the surface of the hydrogel. The PDMS mold was replaced with another PDMS mold that has a thickness of 0.7 mm, and then a clean piece of glass was placed on top. The peptide grating solution was injected between the hydrogel and the new piece of glass and crosslinked on top of the PEG hydrogel under the UV lamp for 7 min. The peptide grafted hydrogel was then rinsed and swollen in sterile PBS for experiments.

3.3.8 6x Histidine Tag Characterization

After acryloyl-PEG-6His-RGDS was grafted on PEGDA hydrogel, the hydrogel was swollen in sterile PBS. A hole punch was used to punch out a disk shape of the hydrogel and placed into wells of flat bottom black 96-well plate. Anti-6His-FITC antibody was diluted in 1:200 in sterile PBS and was added 75 μL into each well for incubation at room temperature for 4 hrs. After incubation, the antibody was removed

and 150 μL of blocking buffer (3% FBS in PBS) was added to soak the hydrogel three times with 1 hour each in the dark at room temperature. Then each hydrogel was rinsed twice with sterile PBS and 100 μL of PBS was added into each well. Fluorescence intensity was observed by microplate reader (Synergy HT, Biotek). Optics position was set to the top with the excitation/emission wavelengths to be 485/528 nm.

3.4 Cell Adhesion on Peptide Grafted Hydrogel

To determine the grafting of peptide on hydrogel, cell adhesion study was performed. After the hydrogel was formed and swollen, ECFCs were seeded on the hydrogel at a seeding density of 30,000 cells/mL and incubated at 37°C and 5% CO_2. After 1 hour of incubation, the hydrogel was rinsed with sterile PBS and images were taken under microscope.

3.5 Dynamic Adhesion

When ECFCs reached 90% confluence, ECFCs were detached from culture flask and resuspended in ECFC media to reach a final concentration of 1 x 10^6 cells/mL with the use of a hemocytometer to determine cell density. Cell suspension was added into a 10 mL syringe (BD) that served as a cell reservoir, and the cell reservoir was placed within a 50 mL centrifuge tube that served as a water jacket controlling at 37°C by an in-line heater controller (TC324B, Warner Instrument Corporation). The water to the water jacket was recycled by a peristaltic pump (Masterflex). Cell suspension was constantly stirred at 150 rpm before the start of the flow and between runs to minimize cell settling and aggregation. A low-flow syringe pump (Legato 180, KD Scientific) was used to create the various shear rates by withdrawing cell suspension from the reservoir through the flow chamber. The syringe pump was raised to maintain the same level as the flow

chamber positioned on the stage of an inverted microscope. Hydrogel was placed on a 2 in x 3 in glass slide (VWR) and flow deck was then placed on top of the hydrogel. A PDMS ring was placed on the glass slide to contain flow media from dripping into the interior of the microscope if a leak were to occur. Two metal plates and screws were used as a clamp to hold the flow chamber, hydrogel and glass slide together. The flow chamber was placed on the phase contrast microscope (Ti Eclipse, Nikon). Video recording of ECFC rolling was performed with an Andor Luca S high speed camera at 70 fps on a 20X objective. The full setup is shown in Figure 24.

Figure 24: Image of dynamic adhesion setting. A 10 mL syringe without the plunger was used as cell reservoir. Cell reservoir was placed in a 50 mL centrifuge tube that served as a water jacket to control temperature by an in-line water heater. Cells were withdrawn from the cell reservoir through the flow chamber by a syringe pump on the left. The chamber setup was placed on the microscope stage that was connected to a high speed camera for video recording.

3.6 Migration of ECFCs on Peptide-Grafted Hydrogel

To study the migration of ECFCs on the hydrogel surface, a migration assay was developed which provided a stable seeding and tracking environment. First, glass slides were acrylated by first soaking them in piranha solution which was prepared by mixing 70% sulfuric acid (J.T.Baker) and 30% hydrogen peroxide (EMD) in a glass staining dish (VWR) for 10 min, then following a rinse with ethanol. The cleaned glass slides were placed in an oven at 100°C until dry and incubated in acrylation solution at room temperature overnight. The acrylation solution was prepared by mixing 3% 0.2 N acetic acid, 0.5% 3-(trimethoxysilyl)propyl methacrylate (Sigma) in ethanol. The acrylated glass slides were rinse with ethanol and dried in the oven at 100°C . The glass slides were covered with foil and then transferred into biosafety cabinet before use.

Crosslinking the hydrogel onto the acrylated glass slide was done in a very similar manner to the creation of hydrogels that were not crosslinked to glass slide as described above, except an acrylated glass slide was used. After crosslinking under UV, PEG hydrogel in contact with the acrylated glass slide was covalently bonded to the acrylated glass slide. Then the grafting peptide can be grafted on the other side. The glass slide with the hydrogel coupled was placed in a slide dish with sterile PBS to swell the peptide grafted hydrogel.

After swelling, the PBS is removed and a PDMS migration mold was placed on top of the hydrogel to create a seeding area for ECFCs. A plastic grid with metal plates and screws was used to prevent the PDMS migration mold from sliding. An image of the setup and a schematic of the PDMS migration mold on top of hydrogel are shown in

Figure 25. ECFCs were detached and seeded into the seeding area at 30,000 cells/cm^2. The cells were allowed to adhere and grow to confluent at 37°C with 5% CO_2 for 24 hr.

The migration mold was then removed and the hydrogel was marked with a blade to indicate the start edge of the cell seeding area. ECFCs were rinsed twice with warm PBS and ECFCs media was added. Images of the edge of the cell seeding area were taken to serve as a record for the starting point of migration and cells were allowed to migrate. Migration distance was recorded by taking pictures every day over the course of 3 days.

3.7 Statistical Analysis

Results were presented as average of three or more replicates of experiment. Statistical analysis was reported in terms of P values from t-test.

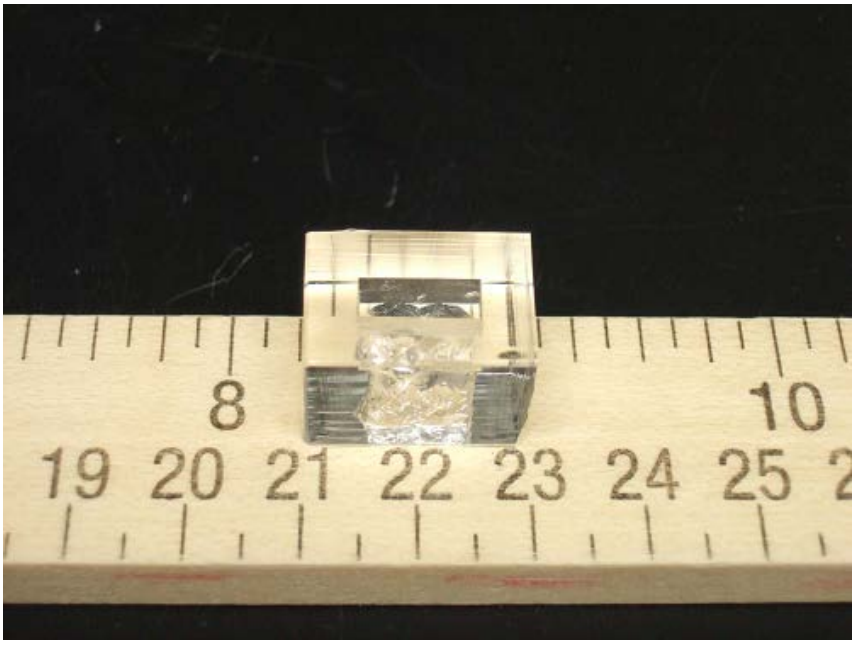

a)

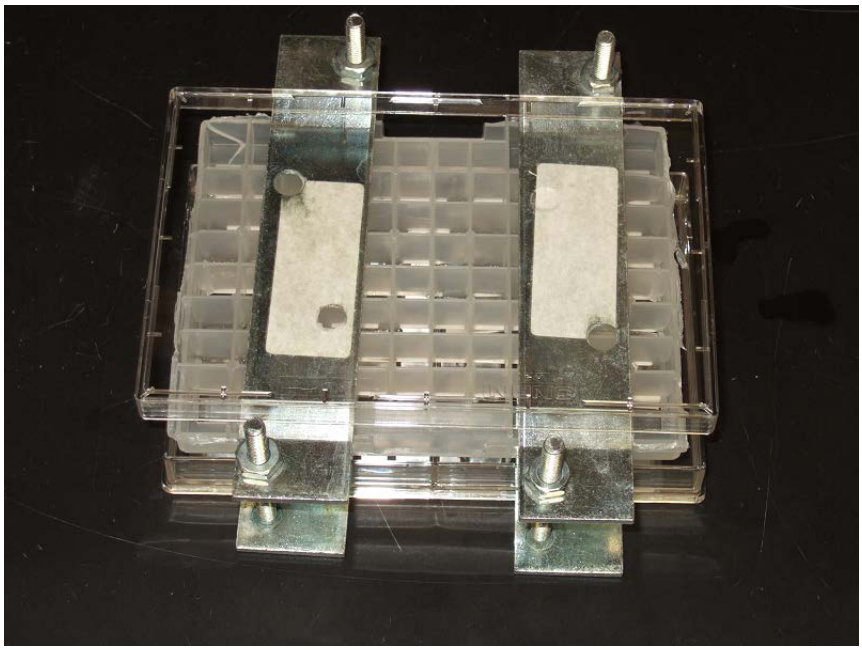

b)

Figure 25: Setup for ECFC migration study. a) PDMS seeding mold used to create a restricted cell seeding area. b) After hydrogel on acrylated glass was placed into the dish, PDMS seeding mold was placed on top of the hydrogel. A plastic grid was placed on top and held together by metal plates and screws.

4. RESULTS AND DISCUSSION

4.1 The Effect of Photoinitiator on ECFC Viability

In order to select the optimal photoinitiator to crosslink PEGDA, a cell viability assay of four photoinitiators was performed on ECFCs. Since cell viability was measured as absorbance, the absorbance of ECFCs that were cultured with media only was used as reference. The effect of UV or light exposure for 5 min on the ECFC viability is negligible as shown in Figure 26. Same amount of ethanol that was used in dissolving the photoinitiators was added to the media in order to show the effect of ethanol on cell viability. There is a significant decrease in ECFC viability by the addition of ethanol in the dark and a non-significant decrease after exposure to UV. For I-184 and I-651 (DMPA), both showed that ECFC viability was extremely poor regardless of the concentrations and UV exposure (Figure 26a and Figure 26b). The effect of I-2959 significantly reduced ECFC viability at all concentrations and with or without UV exposure, but the result was far greater than both I-184 and DMPA (Figure 26c). Comparing to the other three photoinitiators, Eosin Y yielded the best result. Without light exposure, there is a slight decrease in viability at concentrations of 0.007% and 0.014%, whereas a non-significant decrease in viability is shown with light exposure (Figure 26d). Therefore, Eosin Y produced the best result in terms of ECFC viability.

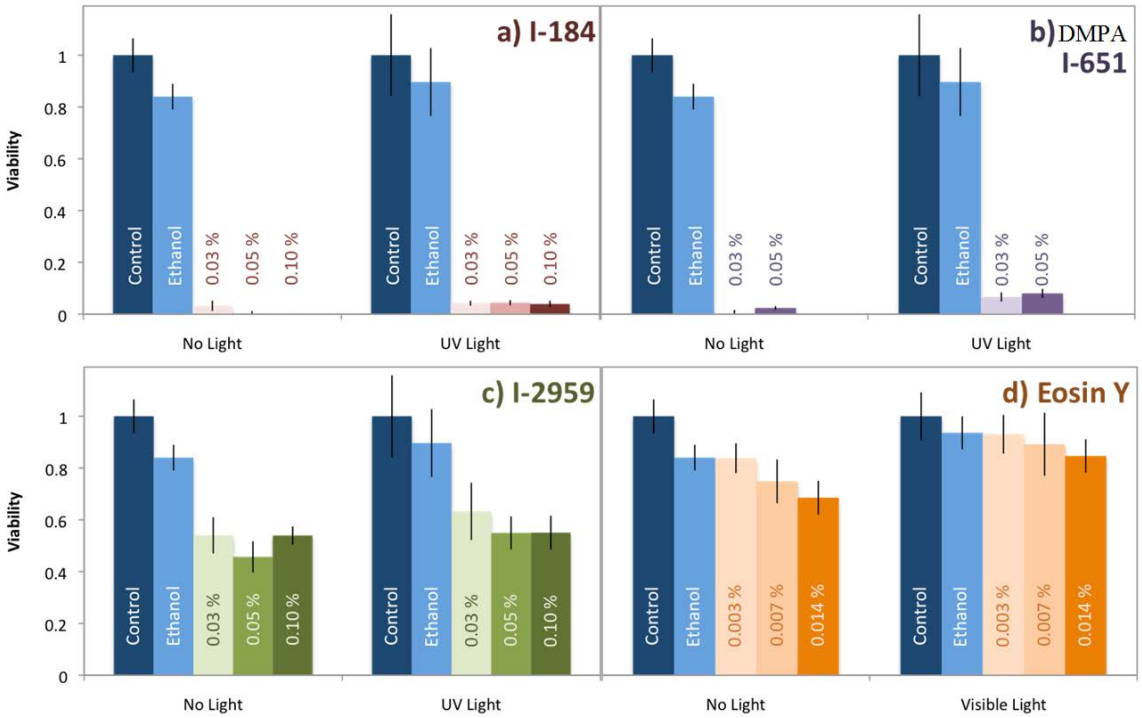

Figure 26: ECFCs in culture with exposure to photoinitiators. A decreased viability is shown when ECFCs are exposed to (a) I-184 or (b) DMPA. This effect was alleviated with (c) I-2959 and (d) Eosin Y.

Besides cell viability, other considerations were also taken into account seriously in photoinitiator selection. As discussed in Section 2.4.4, Eosin Y is fluorescent in the FITC range and affects the performance of immunostaining, so Eosin Y was not compatible with anti-6H-FITC antibody in the characterization of peptide grafting study. Moreover, it was also not compatible with the most common Live/Dead immunostaining. Although I-2959 gave better viability result comparing to I-184 and DMPA, it had a hard time in crosslinking PEGDA in to hydrogel using 365 nm UV light unless using a shorter wavelength UV light that has potential in being mutagenic. Thus, I-2959 possessed safety issue. Similarly, I-184 has a weak crosslinking ability at 365 nm. Therefore, DMPA was chosen as the optimal photoinitiator for crosslinking PEGDA with respect to overall

performance. Migration of ECFC on RGDS-grafted hydrogel using DMPA as photoinitiator is shown in Section 4.6 to illustrate the absence of viability issue.

4.2 The Effect of Glass Cleaning Method on PEG Hydrogel Formation

During grafting of peptides on PEG hydrogel, a small amount of peptide residues was suspected to be left on the glass surface. Wiping with ethanol alone may not be enough to clean the glass, so a qualitative study was performed to determine whether there were peptide residues left on the glass surface. Three methods were used to clean the glass surface such as wiping with ethanol, brushing with glass soap and soaking in base bath. After cleaning with one of the methods, the glass slides were used to prepare PEG hydrogel and ECFCs were seeded on the PEG hydrogel. Results showed that ECFCs were fully adhered and spread on PEG hydrogels that were prepared by using ethanol cleaned glass (Figure 27a). ECFCs on PEG hydrogel prepared by glass soap washed glass showed minimal adhesion and slight spreading (Figure 27b). For PEG hydrogel that were prepared by the glass that were soaked in base bath, there were minimal ECFCs adhesion but no spreading (Figure 27c). This result was very surprising on how the acryloyl-PEG-peptide were left on non-acrylated glass surface and then the residues were able to be transferred to PEG hydrogel surface. Therefore, soaking the glass slides with base bath is critical in the preparation of clean glass surface for PEGDA crosslinking in order to avoid compromising the grafting quality.

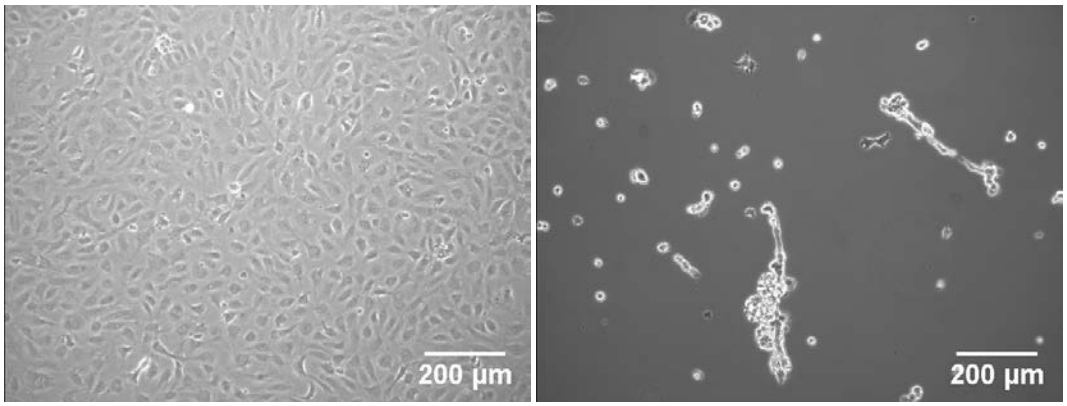

a) b

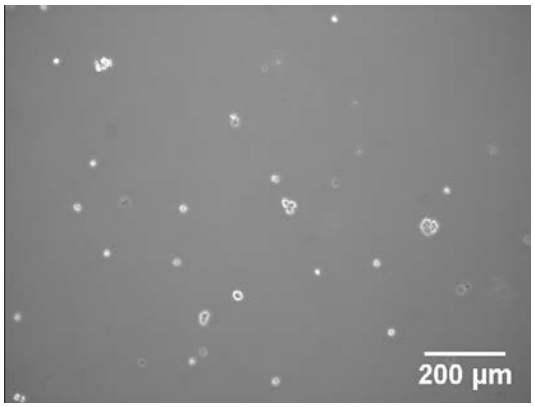

c)

Figure 27: PEGhydrogel was made by glass that were cleaned with different methods. a) ECFCs were able to adhere and spread on PEG hydrogel made with ethanol cleaned glass. b) Some spreading was shown on PEG hydrogel made with glass cleaned with glass soap. c) No spreading and only minimal ECFC adhesion was shown on PEG hydrogel made with glass cleaned with base bath.

4.3 The Effect of Grafting Time for Successful Peptide Grating on PEG Hydrogel

Optimal UV exposure time for grafting of peptides on PEG hydrogel was studied. As shown by Taite *et al.*, an UV exposure of 1 min was used with an UV lamp having 10 mW/cm^2 at 365 nm [79]. However, this time of UV exposure was found to be insufficient to graft acryloyl-PEG-peptides on PEG hydrogel in this study. Three different UV exposure times were studied: 30 s, 2 min, and 7 min. After grafting the acryloyl-PEG-RGDS (1.4 µmol/mL) on PEG hydrogel with different UV exposure time, ECFCs

were seeded on the surfaces and allowed to adhere for 1.5 hr. Then the number of adherent cells were counted. These cells were allowed to proliferate and counted after 40 hr. The number of ECFCs on the PEG hydrogel decreased significantly as expected; PEG is known to resist protein adsorption and cell adhesion, so the loosely adhering ECFCs were washed off during the PBS rinsing. The number of ECFCs on the hydrogels grafted showed a decreased in number for 30 s and 2 min. This was probably because of incomplete grafting of the acryloyl-PEG-RGDS. On the hydrogel with the grafting time of 7 min, ECFCs showed spreading at 1.5 hr after seeding and the number of ECFCs increased significantly 40 hr later (Figure 28). Therefore, a grafting time of 7 min was necessary to show complete grafting. Another study was performed using 2.8 μmol/mL of acryloyl-PEG-RGDS to evaluate a higher peptide concentration affects the needed grafting time. Figure 29 shows no significant differences in the number of cells on the hydrogels grafted with two different concentrations of peptide solution at time equals 41.5 hr. There were no significant difference. Therefore, a grafting time of 7 min was used for all conditions.

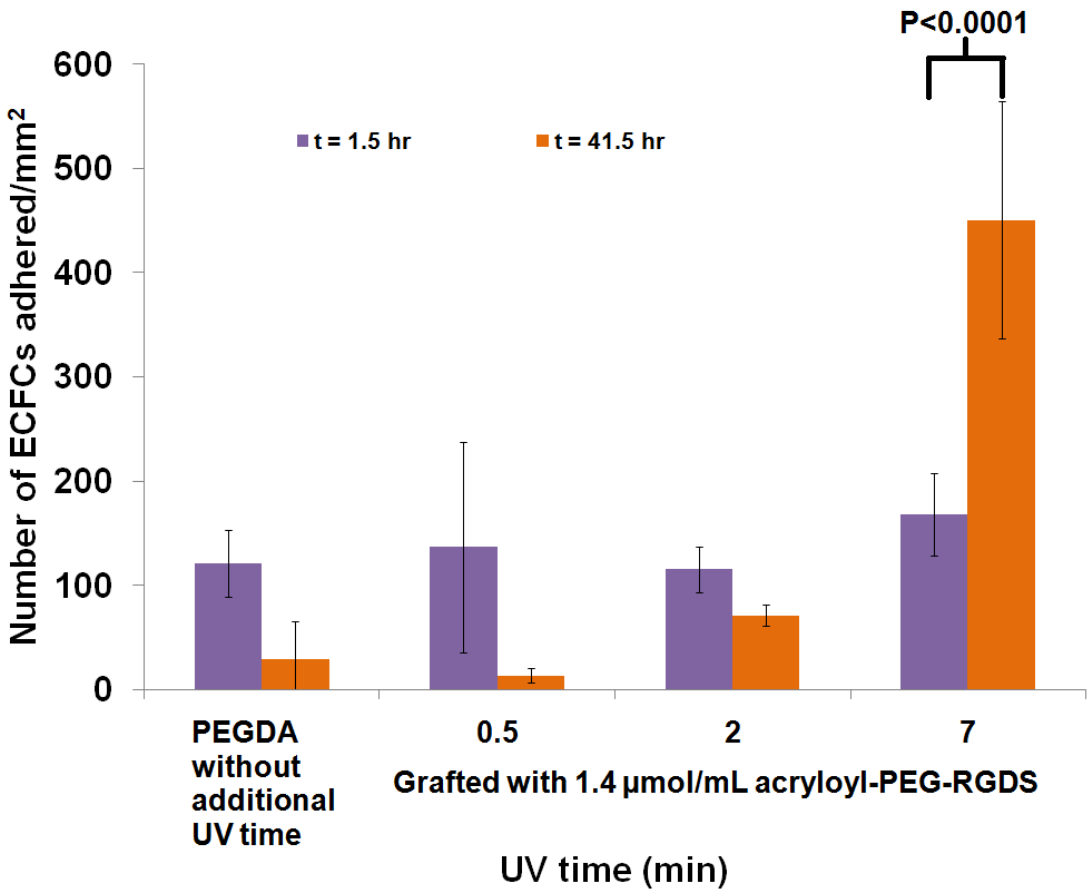

Figure 28: The effect of UV time on successful grafting of RGDS peptide. The number of ECFCs adhered significantly decreased on the RGDS-grafted hydrogel with 0.5 and 2 min grafting time after 40 hours whereas the number of ECFCs increased significantly on the RGDS-grafted hydrogel with 7 min grafting time after 40 hours. This showed that grafting of RGDS was completed with a grafting time of 7 min in terms of number of ECFCs adhered on the hydrogel.

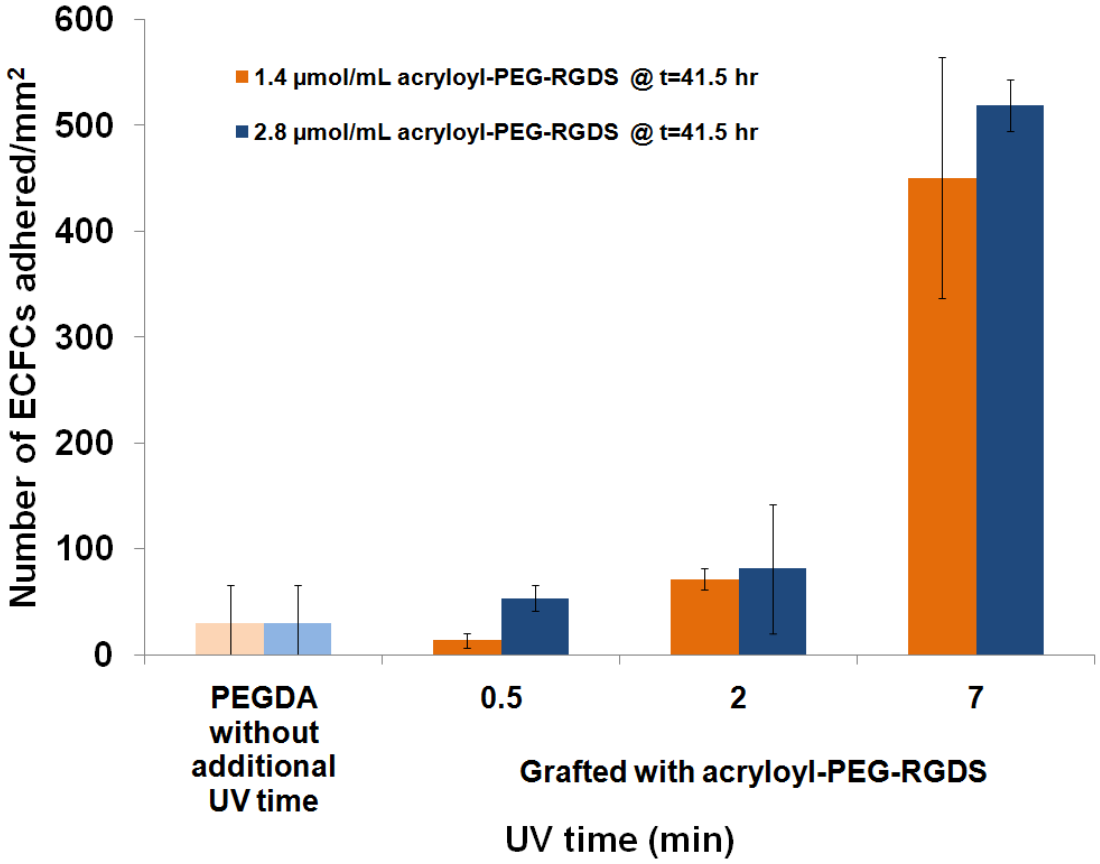

Figure 29: The effect of UV time on different concentrations of grafting RGDS peptide. The number of ECFCs adhered on RGDS-grafted hydrogel using after 40 hours showed no significant difference between using 1.4 µmol/mL or 2.8 µmol/mL acryloyl-PEG-RGDS solution. This showed that the increase in the concentration of acryloyl-PEG-RGDS solution did not affect the grafting of RGDS with a grafting time of 7 min in terms of number of ECFCs adhered on the hydrogel.

4.4 Confirmation of Peptide-Grafting by 6x Histidine Tagged Immunostaining

Grafting method used in this study is further confirmed using immunostaining. Due to the use of free radical chemistry in grafting peptide on PEG hydrogel, termination step can cause the joining of $CH_2\cdot$ on PEGDA and limit the availability of acrylate end groups on PEG hydrogel for grafting. Therefore, it was necessary to verify the success of

acryloyl-PEG-peptide grafting. After grafting the acryloyl-PEG- HHHHHHRGDSG onto PEG hydrogel, immunostaining by anti-6His-FITC antibody allows the surface of the grafted hydrogel to fluorescence under UV. The intensity of fluorescence can be used as a quantitative means to estimate the relative amount of peptide that was grafted on the surface. The concentration of 0.7 μmol/mL of acryloyl-PEG-HHHHHHRGDSG was used due to the observation where it is the minimum concentration required to support ECFCs spreading. Therefore, 2.8 and 5.6 μmol/mL were tested due to the reason of being four times and eight times of 0.7 μmol/mL respectively. Ungrafted PEG hydrogel was used as control.

As shown in Figure 30, the averaged normalized fluorescence intensity in each condition was determined by subtracting the value of the control. For the hydrogel that used 0.7 μmol/mL of acry-PEG-6HRGDS in the grafting solution, intensity was found to be 121 (P<0.05). For 2.8 and 5.6 μmol/mL of acry-PEG-HHHHHHRGDSG, the intensities were 400 (P<0.06) and 536 (P<0.01) respectively. Besides the confirmation of the presence of the peptides on the hydrogel, the result also showed the increase in intensity with respect to the increase in concentration of grafting solution. The fluorescence intensity was found to be significantly higher in 5.6 μmol/mL than 0.7 μmol/mL (P<0.03). This result also suggested that acryloyl-PEG-peptide can be grafted on the surface of PEG hydrogel in a concentration dependent fashion using photopolymerization.

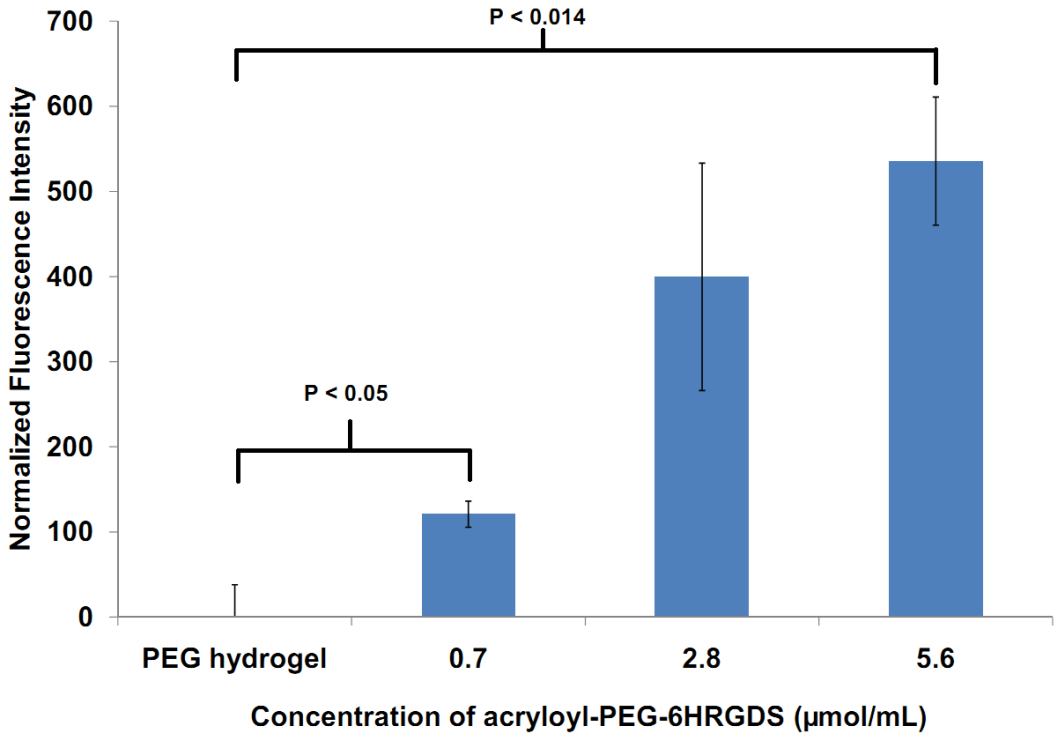

Figure 30: Grafting of peptide on PEG hydrogel was verified by immunostaining. The immunostaining also showed an increase of fluorescence intensity with respect to the concentration of acryloyl-PEG-6HRGDS solution.

4.5 ECFCs Rolling on Peptide-Grafted Hydrogel

4.5.1 No ECFCs Rolling on PEG Hydrogel

To understand the dynamic adhesion of ECFCs on hydrogel, rolling of ECFCs was investigated in terms of cell rolling velocity [60]. ECFCs single-cell suspension was flowed through the surface on PEG hydrogel at shear rates of 20 s^{-1}, 40 s^{-1}, 80 s^{-1}, and 120 s^{-1}. Video recordings showed that ECFCs rotation was observed and cell tracking showed that ECFCs rolled at a lower speed comparing to the estimated fluid velocity at the height of average diameter of ECFCs, which is 15 µm, in suspension (Figure 31). Since PEG hydrogel did not support ECFCs adhesion as shown in Section 4.3, ECFCs are not supposed to roll on PEG hydrogel. Therefore, it is believed that there were non-

specific interactions that caused the reduction in rolling velocity. This rolling velocity was used in determining the cutoff for rolling velocity in other conditions as suggested by literature [60]. A cutoff of 40% of average fluid velocity was used to be used for cell tracking and is shown in Figure 31.

The choice of 40% of average flow velocity as the cutoff is further validated by comparing to the instantaneous velocity of ECFCs rolling on PEG hydrogel. A representative plot for instantaneous rolling velocity for an ECFC that was tracked across the field of view at 80 s^{-1} is shown in Figure 32. All instantaneous velocities were above the 40% cutoff. Therefore, a cutoff of 40% of average fluid velocity was showed to be sufficient and was used for future cell tracking.

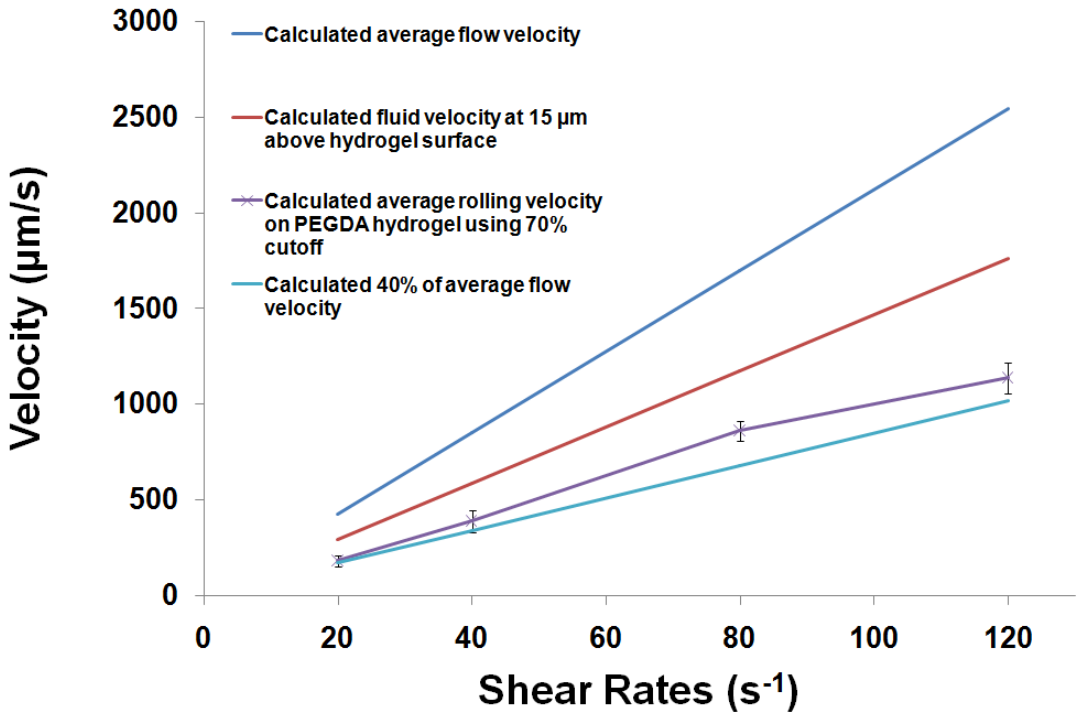

Figure 31: Comparison between calculated fluid velocities and ECFCs rolling velocity. ECFCs rolling on PEG hydrogel was assumed to be a result of non-specific interaction, so a 40% of average fluid velocity was used as a cutoff for identification of rolling cells.

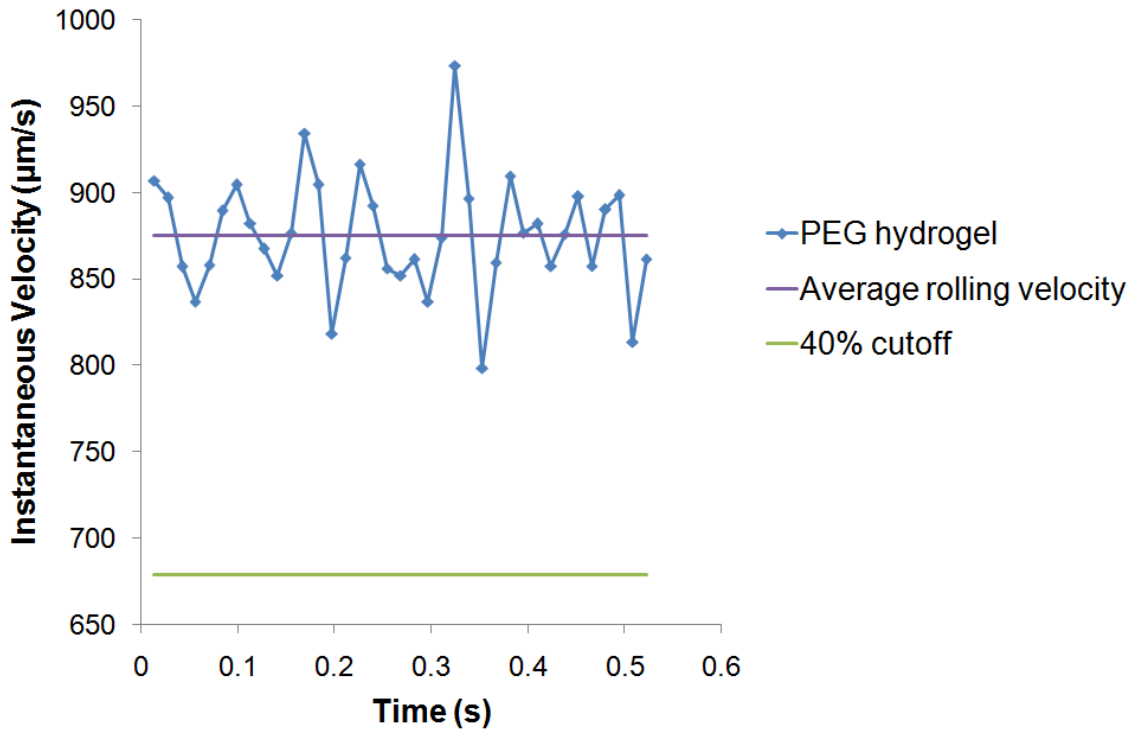

Figure 32: Instantaneous velocity, average rolling velocity and 40% of average fluid velocity of a representative ECFC on PEG hydrogel were shown and compared.

4.5.2 ECFCs Rolling on RGDS-Grafted Hydrogel

As RGDS is the most commonly used cell adhesion peptide, ECFCs rolling on RGDS grafted hydrogel was performed and compared to both PEG hydrogel and RGES grafted hydrogel where RGES was served as a control for RGDS (Figure 33). Rolling velocities of ECFCs on RGES showed no significant difference as compared to PEG hydrogel. On the other hand, rolling velocities of ECFCs on RGDS are significantly decreased comparing to RGES at all shear rates and the rolling velocities were 103 μm/s, 223 μm/s, 469 μm/s, and 741 μm/s at 20 s^{-1}, 40 s^{-1}, 80 s^{-1}, and 120 s^{-1} respectively (P<0.05 for all conditions). Although some capture events were observed at 20 s^{-1}, the quantity was far less than the number of rolling cells and insufficient for analysis. In summary, the grafting of RGDS hydrogel decreased rolling velocities of ECFCs at all shear rates and specific transient binding between ECFCs and RGDS was demonstrated.

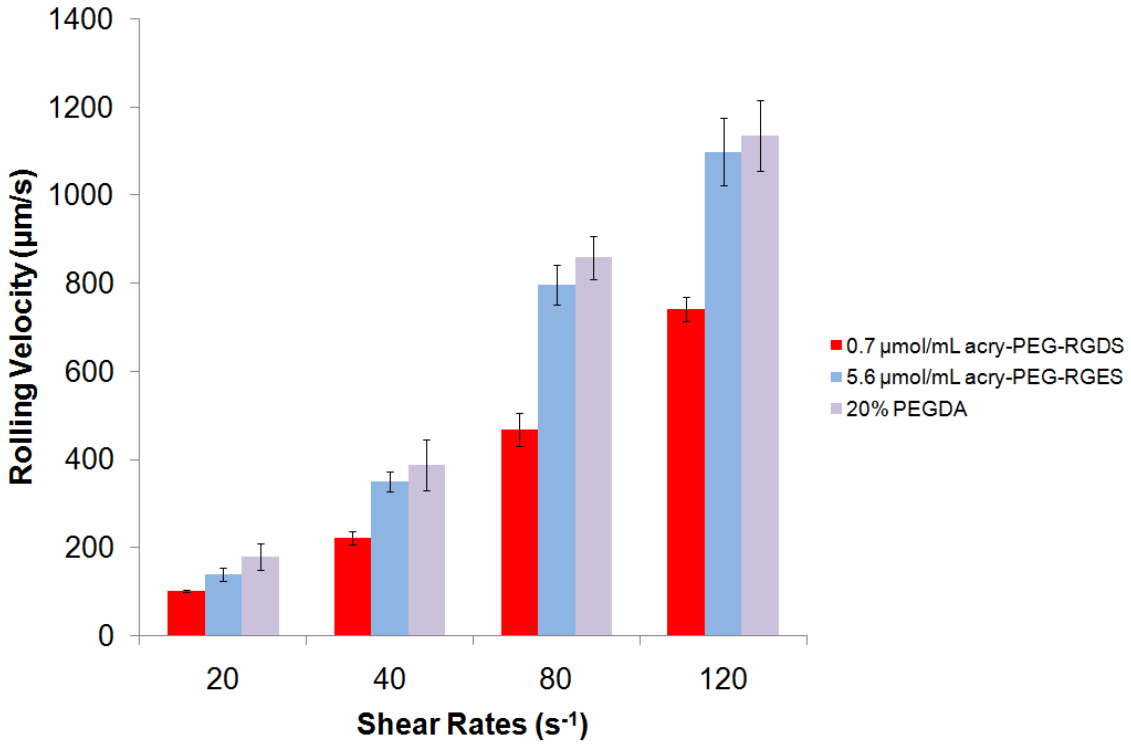

Figure 33: The effect of RGDS-grafted hydrogel on ECFCs rolling velocity. Rolling velocity of ECFCs on RGES-grafted hydrogel was similar to rolling velocity on PEG hydrogel while rolling velocity on RGDS-grafted hydrogel showed significant decrease comparing to RGES-grafted and PEG hydrogel at all shear rates.

4.5.3 ECFCs Rolling on YIGSR and REDV-Grafted Hydrogel

The effect of peptide on ECFCs rolling velocity was further demonstrated by rolling ECFCs on YIGSR and REDV grafted hydrogels. Rolling velocities on YIGSR showed similar result to RGDS (Figure 34) and the rolling velocities were 102 μm/s, 223 μm/s , 484 μm/s, and 740 μm/s at 20 s^{-1}, 40 s^{-1}, 80 s^{-1}, and 120 s^{-1} respectively. In contrast, REDV grafted hydrogel further reduced ECFCs rolling velocities as compared to both RGDS and YIGSR (Figure 34). The rolling velocities were 79 μm/s, 181 μm/s, 357 μm/s, and 560 μm/s at 20 s^{-1}, 40 s^{-1}, 80 s^{-1}, and 120 s^{-1} respectively (P<0.01 for all conditions comparing to RGDS). This result showed that YIGSR do support ECFCs

rolling to the similar extend with RGDS, while the significant decrease in ECFCs rolling velocity by REDV showed that ECFCs rolling on hydrogel depends on the peptide grafted.

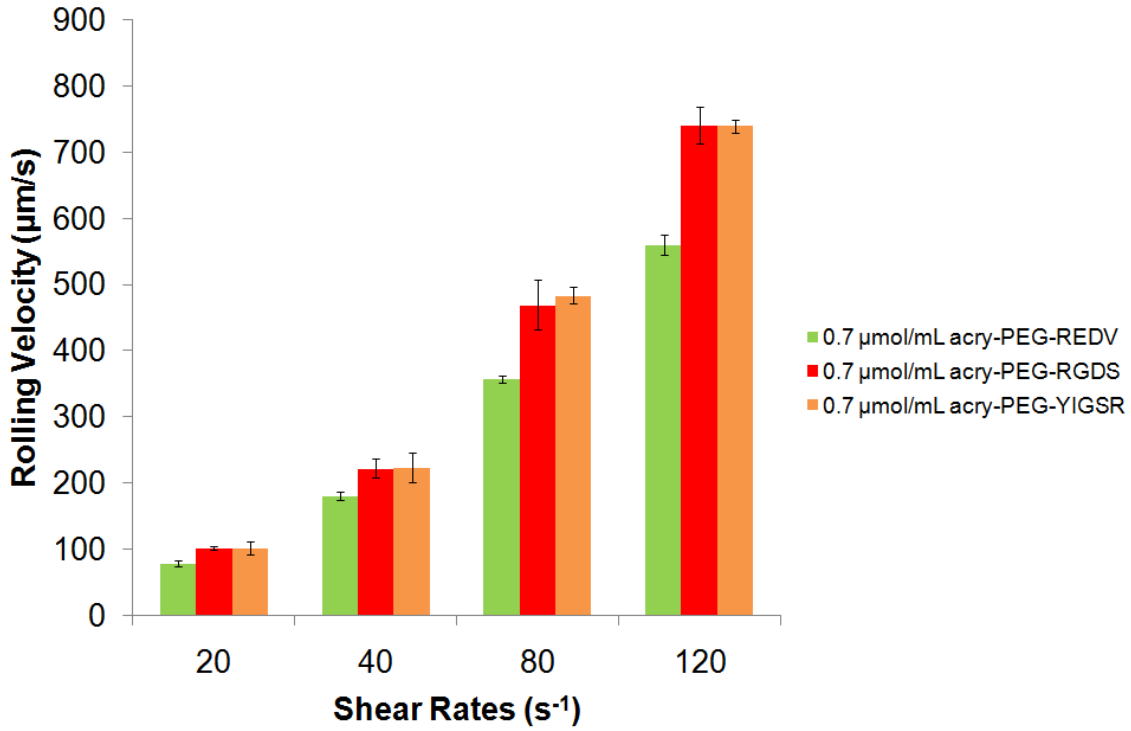

Figure 34: Comparison of the effect of REDV, RGDS, and YIGSR-grafted hydrogel on ECFCs rolling velocity. ECFCs showed reduced rolling velocity on REDV-grafted hydrogel ($P<0.01$).

4.6 ECFCs Migration on Hydrogel

Migration of ECFCs on the surface of peptide-grafted hydrogel was quantitatively studied in terms of migration distance. Two conditions were studied which were 2.8 μmol/mL acryloyl-PEG-RGDS (Figure 35a-c) and 2.8 μmol/mL of a mixture of 1:1 mol ratio of acryloyl-PEG-RGDS and acryloyl-PEG-YIGSR (Figure 35d-f). After removal of the PDMS seeding mold, a sterile X-acto knife was used to create markings on the hydrogel to serve as reference points. The reference points were linked by a black solid line as shown in Figure 35 and the black solid line was used to line up the images at

different time points for comparison. Images were taken right after the removal of PDMS seeding mold (Figure 35a & d), 24 hours (Figure 35b & e) and 72 hours (Figure 35c & f). Positions of ECFCs that were on the leading edge were recorded in order to calculate the average migration distance. Results are shown in Figure 36. At 24 hour, ECFCs on RGDS only hydrogel surface have migrated an average of 293 μm, while ECFCs on the mixture of RGDS and YIGSR hydrogel surface have migrated 314 μm. At 72 hour, ECFCs on RGDS only hydrogel surface have migrated 864 μm, while ECFCs on the mixture of RGDS and YIGSR hydrogel surface have migrated 884 μm. The migration distance of 50-100 of ECFCs with triplicates (n=3) was measured. Although YIGSR is supposed to enhance endothelial migration, no significant difference was found between the two conditions. As the peptides were grafted on the PEG hydrogel surface without any gradient, this did not provide polarity towards a directional migration. Therefore, there were no significant differences between the conditions.

In terms of migration distance, Jun *et al.* has performed similar study investigating the migration of bovine aortic endothelial cells on YIGSR/PEG modified polyurethane urea film. Although only migration over the boundary was reported in their study, BAECs had migrated a distance of about 150 μm after 24 hours and 290 μm after 48 hours by visually estimating Figure 37. In comparison to the result in this study, ECFCs have shown excellent migration on the two hydrogel formulations studied.

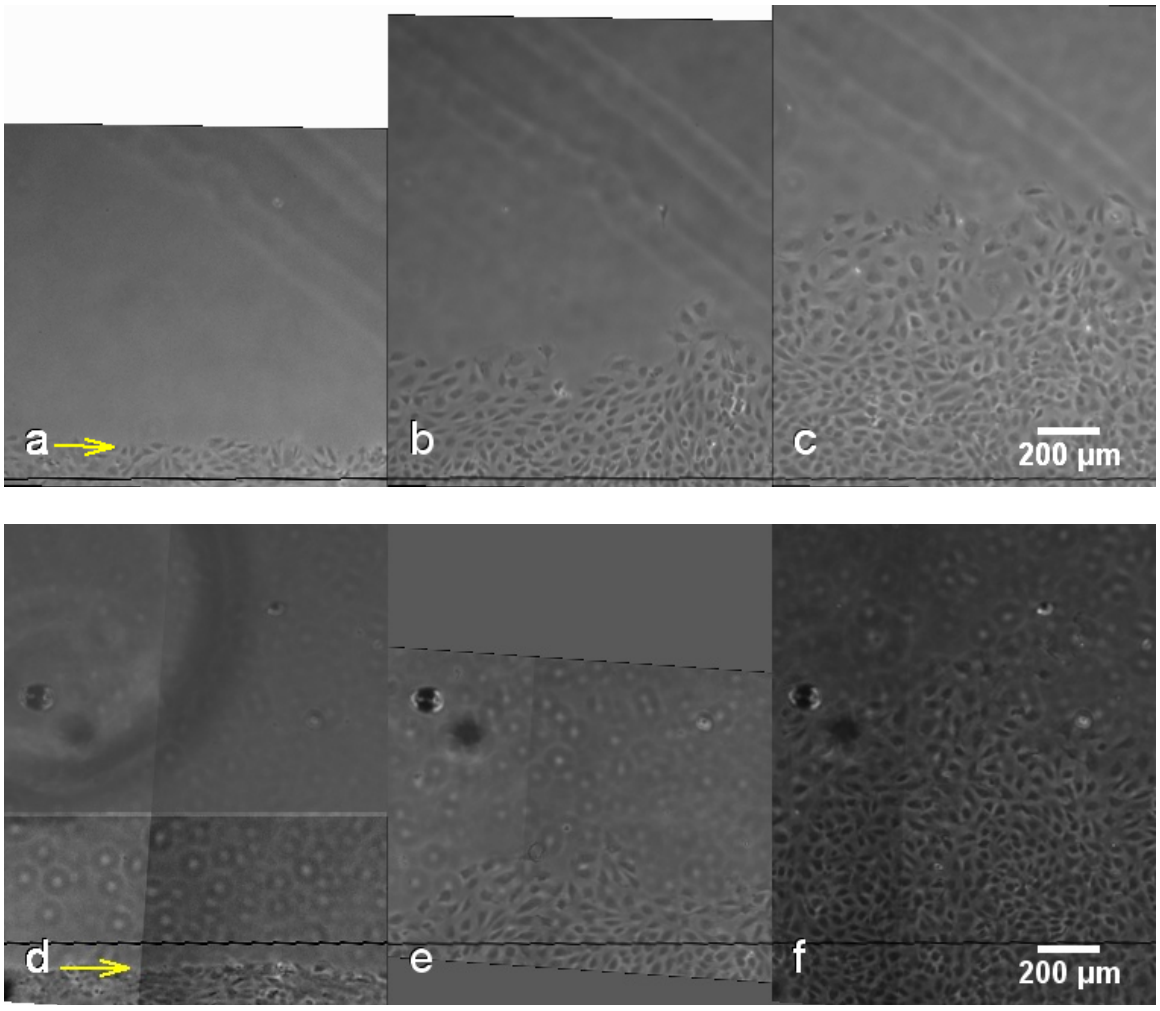

Figure 35: ECFC migration on hydrogels. ECFC migration on RGDS-grafted hydrogel a)-c) and on YIGSR/RGDS-grafted hydrogel d)-f). Yellow arrow indicated the original boundary. Black line was used to line up the micrographs at different time points. a) & d) at time = 0 hour, b) & e) at time= 24 hours, and c) & f) at time = 72 hours.

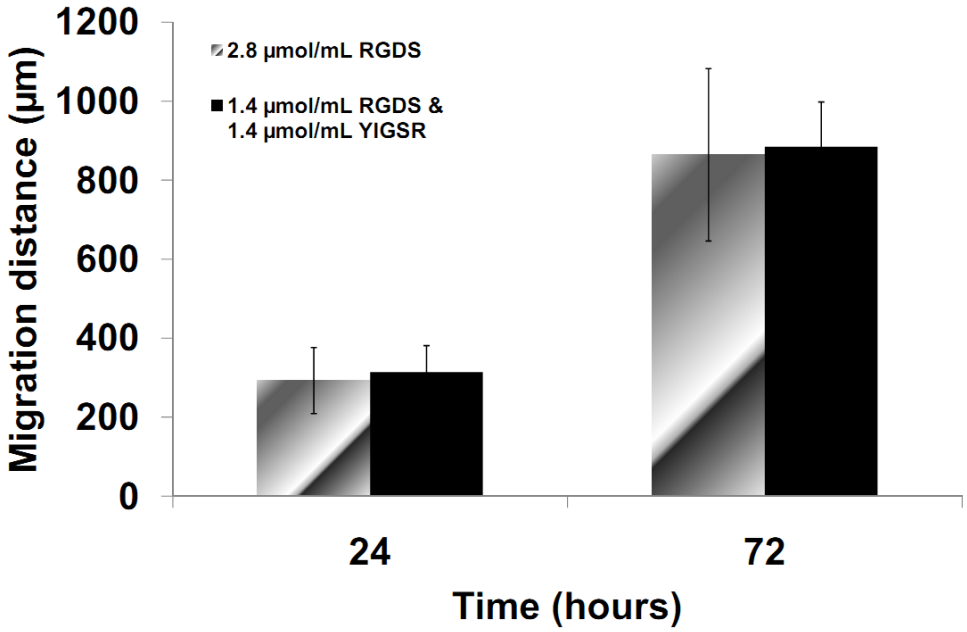

Figure 36: No difference was found between the effect of RGDS-grafted and YIGSR/RGDS-grafted hydrogel on ECFCs migration distance at 24 hours and 72 hours.

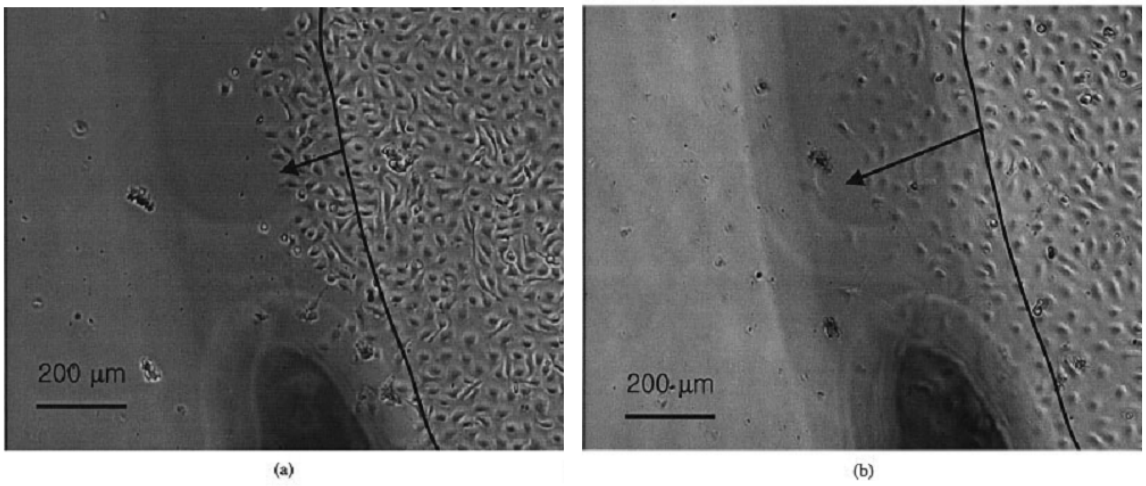

Figure 37: Migration of BAECs on YIGSR/PEG modified polyurethane urea film after 24 hours (a) and 48 hours (b). Reprinted with permission from Ref 39.

5. CONCLUSIONS

Endothelial progenitor cells have been shown to have great potential in performing re-endothelialization which demonstrate a promising autologous cell source for clinical applications. Endothelial colony forming cells are the type of EPC that have high proliferative potential for rapid endothelialization and is the major interest in this study. Another main focus in this study was to design and prepare a biomaterial for ECFCs. Peptide-grafted hydrogels have been developed and the preparation steps were evaluated carefully, including photoinitiator selection, glass cleaning methods for hydrogel polymerization, UV exposure time for successful peptide grafting, and grafting confirmation by immunostaining. Development of the cell tracking system for rolling cells on hydrogel surfaces was another core achievement of this study. With this new approach, tracking of rolling cells on hydrogels is much more efficient and productive. The position identification by ImageJ and the matching process by MATLAB algorithms decreased the tracking time from days to minutes. This facilitates future cell rolling studies in which numerous peptides are of interest for testing. The development of the custom migration assay was also important in determining an accurate migration distance on hydrogel surfaces.

First of all, this study demonstrated that PEG hydrogel do not support ECFC adhesion and rolling. This proves that hydrogels formed with PEGDA provides a "blank slate" for ECFCs as a biomaterial. By grafting peptides onto the PEG hydrogel, ECFCs were able to adhere, roll and migrate on the hydrogel surface. RGDS grafted hydrogels supported ECFC adhesion and rolling. Also, REDV coupled hydrogel showed a significant decrease in rolling velocity as compared to RGDS grafted hydrogels. No

significant differences was found in the migration of ECFCs on YIGSR/RGDS grafted hydrogels and ECFCs showed similar rolling velocity on RGDS grafted hydrogels and YIGSR grafted hydrogels.

6. RECOMMENDATIONS and FUTURE WORK

Since this study has developed an efficient tracking system for ECFC rolling, the effect of different peptides, or different combinations of peptides, on ECFCs rolling can be further studied and analyzed easily. As REDV-grafted hydrogel showed a significant decrease in rolling velocity, further study in endothelial integrin specific peptides may yield fruitful results. In addition to integrins, VE-cadherin may be an alternative possibility for study in ECFC rolling as research has shown that it is exclusively expressed in the late EPCs and ECs, but not on the early EPCs and other leukocytes [45]. Activation of ECFCs may also have great potential to further reduce rolling velocities. Some options that are reported in literatures are VEGF, $MnCl_2$ [13], and statin [33]. Strength of adhesion of ECFCs may be studied after ECFCs are allowed to adhere for a short period of time, for example, for two minutes. By using dextran, viscosity of the flow media can be increased in order to increase shear stress.

With respect to migration, research study has shown that strong cell-cell adhesion inhibits cell migration [43]. So addition of VEGF may be used to disrupt cell-cell adhesion as shown by Weis *et al*. [85,86]. The development of the custom migration assay provides a means to create a restricted cell seeding area on hydrogel surfaces which can be used to study migration of ECFCs on hydrogels under flow. This allows us to study the combination of chemotaxis and mechanotaxis of ECFCs due to the effect by peptides and shear.

REFERENCES

1. Achneck, H. E., R. M. Jamiolkowski, A. E. Jantzen, J. M. Haseltine, W. O. Lane, J. K. Huang, L. J. Galinat, M. J. Serpe, F.-H. Lin, M. Li, A. Parikh, L. Ma, T. Chen, B. Sileshi, C. a Milano, C. S. Wallace, T. V. Stabler, J. D. Allen, G. a Truskey, and J. H. Lawson. The biocompatibility of titanium cardiovascular devices seeded with autologous blood-derived endothelial progenitor cells: EPC-seeded antithrombotic Ti implants. *Biomaterials* 32:10-8, 2011.

2. Acton, S. T., K. Wethmar, and K. Ley. Automatic tracking of rolling leukocytes in vivo. *Microvascular Research* 63:139-48, 2002.

3. Angelos, M. G., M. a Brown, L. L. Satterwhite, V. W. Levering, N. T. Shaked, and G. a Truskey. Dynamic adhesion of umbilical cord blood endothelial progenitor cells under laminar shear stress. *Biophysical Journal* 99:3545-54, 2010.

4. Asahara, T., T. Murohara, a Sullivan, M. Silver, R. van der Zee, T. Li, B. Witzenbichler, G. Schatteman, and J. M. Isner. Isolation of putative progenitor endothelial cells for angiogenesis. *Science (New York, N.Y.)* 275:964-7, 1997.

5. Avci-Adali, M., A. Paul, G. Ziemer, and H. P. Wendel. New strategies for in vivo tissue engineering by mimicry of homing factors for self-endothelialisation of blood contacting materials. *Biomaterials* 29:3936-45, 2008.

6. Avci-Adali, M., G. Ziemer, and H. P. Wendel. Induction of EPC homing on biofunctionalized vascular grafts for rapid in vivo self-endothelialization--a review of current strategies. *Biotechnology Advances* 28:119-29, 2010.

7. Beijk, M. a M., M. Klomp, N. J. W. Verouden, N. van Geloven, K. T. Koch, J. P. S. Henriques, J. Baan, M. M. Vis, E. Scheunhage, J. J. Piek, J. G. P. Tijssen, and R. J. de Winter. Genous endothelial progenitor cell capturing stent vs. the Taxus Liberte stent in patients with de novo coronary lesions with a high-risk of coronary restenosis: a randomized, single-centre, pilot study. *European Heart Journal* 31:1055-64, 2010.

8. Berlec, A., P. Zadravec, Z. Jevnikar, and B. Štrukelj. Identification of candidate carrier proteins for surface display on Lactococcus lactis by theoretical and experimental analyses of the surface proteome. *Applied and Environmental Microbiology* 77:1292-300, 2011.

9. Brown, M. A., C. S. Wallace, P. D, M. Angelos, and G. A. Truskey. Late Outgrowth Endothelial Progenitor Cells Exposed to Laminar Shear Stress. *Tissue Engineering. Part A* 15:, 2009.

10. Caron, A. W., C. Nicolas, B. Gaillet, I. Ba, M. Pinard, A. Garnier, B. Massie, and R. Gilbert. Fluorescent labeling in semi-solid medium for selection of mammalian cells secreting high-levels of recombinant proteins. *BMC Biotechnology* 9:42, 2009.

11. Carter, A. J., M. Aggarwal, G. a Kopia, F. Tio, P. S. Tsao, R. Kolata, A. C. Yeung, G. Llanos, J. Dooley, and R. Falotico. Long-term effects of polymer-based, slow-release, sirolimus-eluting stents in a porcine coronary model. *Cardiovascular Research* 63:617-24, 2004.

12. Chan, L. Y., S. Gunasekera, S. T. Henriques, N. F. Worth, S.-J. Le, R. J. Clark, J. H. Campbell, D. J. Craik, and N. L. Daly. Engineering pro-angiogenic peptides using stable, disulfide-rich cyclic scaffolds. *Blood* 118:6709-17, 2011.

13. Chavakis, E., A. Aicher, C. Heeschen, K.-ichiro Sasaki, R. Kaiser, N. El Makhfi, C. Urbich, T. Peters, K. Scharffetter-Kochanek, A. M. Zeiher, T. Chavakis, and S. Dimmeler. Role of beta2-integrins for homing and neovascularization capacity of endothelial progenitor cells. *The Journal of Experimental Medicine* 201:63-72, 2005.

14. Choi, W. S., W. J. Bae, Y. K. Joung, and K. D. Park. Fabrication of EC-Specific PU surfaces co-immobilized with GRGDS and YIGSR Peptides. *Macromolecular Research* 17:458-463, 2009.

15. DiVietro, J. a, M. J. Smith, B. R. Smith, L. Petruzzelli, R. S. Larson, and M. B. Lawrence. Immobilized IL-8 triggers progressive activation of neutrophils rolling in vitro on P-selectin and intercellular adhesion molecule-1. *Journal of Immunology (Baltimore, Md. : 1950)* 167:4017-25, 2001.

16. Dijkgraaf, I. Application of RGD-containing peptides as imaging probes for alphavbeta3 expression. *Frontiers in Bioscience* 887, 2009.

17. Fiji. Auto Threshold. , 2011.at <http://fiji.sc/wiki/index.php/Auto_Threshold>

18. Fischman, D. L., M. B. Leon, D. S. Baim, R. A. Schatz, M. P. Savage, I. Penn, K. Detre, and L. Veltri. A Randomized Comparison of Coronary-Stent Placement and Balloon Angioplasty in the Treatment of Coronary Artery Disease. *The New England Journal of Medicine* 331:496-501, 1994.

19. Fittkau, M. H., P. Zilla, D. Bezuidenhout, M. P. Lutolf, P. Human, J. a Hubbell, and N. Davies. The selective modulation of endothelial cell mobility on RGD peptide containing surfaces by YIGSR peptides. *Biomaterials* 26:167-74, 2005.

20. Frangos, J. A. ., S. G. . Eskin, L. V. . McIntire, and C. . L. . Ives. Flow Effects on Prostacyclin Production by Cultured Human Endothelial Cells. *Advancement Of Science* 227:1477-1479, 1985.

21. Garg, S., H. J. Duckers, and P. W. Serruys. Endothelial progenitor cell capture stents: will this technology find its niche in contemporary practice? *European Heart Journal* 31:1032-5, 2010.

22. Genové, E., C. Shen, S. Zhang, and C. E. Semino. The effect of functionalized self-assembling peptide scaffolds on human aortic endothelial cell function. *Biomaterials* 26:3341-51, 2005.

23. Giancotti, F. G. Integrin Signaling. *Science* 285:1028-1033, 1999.

24. Glagov, S. Hemodynamics and atherosclerosis - Insights and perspectives gained form studies of human arteries. *Archives of Pathology & Laboratory Medicine* 112:1018, 1988.

25. Gonzalez, A. L., A. S. Gobin, J. L. West, L. V. McIntire, and C. W. Smith. Integrin interactions with immobilized peptides in polyethylene glycol diacrylate hydrogels. *Tissue Engineering* 10:1775-86, 2004.

26. Graf, J., R. C. Ogle, F. a Robey, M. Sasaki, G. R. Martin, Y. Yamada, and H. K. Kleinman. A pentapeptide from the laminin B1 chain mediates cell adhesion and binds the 67,000 laminin receptor. *Biochemistry* 26:6896-900, 1987.

27. Hern, D. L., and J. a Hubbell. Incorporation of adhesion peptides into nonadhesive hydrogels useful for tissue resurfacing. *Journal of Biomedical Materials Research* 39:266-76, 1998.

28. Herold, D. A., K. Keil, and D. Bruns. Oxidation of polyethylene glycols by alcohol-dehydrogenase. *Biochemical Pharmacology* 38:73-76, 1989.

29. Hillwest, J. L., S. M. Chowdhury, A. S. Sawhney, C. P. Pathak, R. C. Dunn, and J. A. Hubbell. Prevention of postoperative adhesions in the rate by in-situ photopolymerization of bioresorbable hydrogel barriers. *Obstetrics and Gynecology* 83:59-64, 1994.

30. Hirschi, K. K., D. a Ingram, and M. C. Yoder. Assessing identity, phenotype, and fate of endothelial progenitor cells. *Arteriosclerosis, Thrombosis, and Vascular Biology* 28:1584-95, 2008.

31. Hoffmann, R., G. S. Mintz, G. R. Dussaillant, J. J. Popma, A. D. Pichard, L. F. Satler, K. M. Kent, J. Griffin, and M. B. Leon. Patterns and Mechanisms of In-Stent Restenosis: A Serial Intravascular Ultrasound Study. *Circulation* 94:1247-1254, 1996.

32. Hristov, M., W. Erl, and P. C. Weber. Endothelial Progenitor Cells Isolation and Characterization. *Trends in Cardiovascular Medicine* 13:201-206, 2003.

33. Hristov, M., A. Zernecke, E. A. Liehn, and C. Weber. Regulation of endothelial progenitor cell homing after arterial injury. *Thrombosis and Haemostasis* 98:274-277, 2007.

34. Huang, L., P. J. Critser, B. R. Grimes, and M. C. Yoder. Human umbilical cord bloof plasma can replace fetal bovine serum for in vitro expansion of functional human endothelial colony-forming cells. *Cytotherapy* 13:712-721, 2011.

35. Hubbell, J. a, S. P. Massia, N. P. Desai, and P. D. Drumheller. Endothelial cell-selective materials for tissue engineering in the vascular graft via a new receptor. *Bio/technology (Nature Publishing Company)* 9:568-72, 1991.

36. Humphries, M. J. Integrin Structure. *Biochemical Society* 28:311-340, 2000.

37. Hur, J., C.-H. Yoon, H.-S. Kim, J.-H. Choi, H.-J. Kang, K.-K. Hwang, B.-H. Oh, M.-M. Lee, and Y.-B. Park. Characterization of two types of endothelial progenitor cells and their different contributions to neovasculogenesis. *Arteriosclerosis, Thrombosis, and Vascular Biology* 24:288-93, 2004.

38. Jantzen, A. E., W. O. Lane, S. M. Gage, R. M. Jamiolkowski, J. M. Haseltine, L. J. Galinat, F.-H. Lin, J. H. Lawson, G. a Truskey, and H. E. Achneck. Use of autologous blood-derived endothelial progenitor cells at point-of-care to protect against implant thrombosis in a large animal model. *Biomaterials* 32:8356-63, 2011.

39. Jun, H.-W., and J. L. West. Modification of polyurethaneurea with PEG and YIGSR peptide to enhance endothelialization without platelet adhesion. *Journal of Biomedical Materials Research. Part B, Applied Biomaterials* 72:131-9, 2004.

40. Jun, H.-wook, and J. L. West. Development of a YIGSR-peptide-modi ed polyurethaneurea to enhance endothelialization. *Journal of Biomaterials Science. Polymer Edition* 15:73-94, 2003.

41. Kiemeneij, F., P. W. Serruys, C. Macaya, W. Rutsch, G. Heyndrickx, P. Albertsson, J. Fajadet, V. Legrand, P. Materne, J. Belardi, U. Sigwart, a Colombo, J. J. Goy, C. M. Disco, and M. a Morel. Continued benefit of coronary stenting versus balloon angioplasty: five-year clinical follow-up of Benestent-I trial. *Journal of the American College of Cardiology* 37:1598-603, 2001.

42. Ku, D. N. Blood Flow in Arteries. *Annual Review of Fluid Mechanics* 29:399-434, 1997.

43. Lamalice, L., F. Le Boeuf, and J. Huot. Endothelial cell migration during angiogenesis. *Circulation Research* 100:782-94, 2007.

44. Ley, K., P. Gaehtgens, C. Fennie, M. S. Singer, L. a Lasky, and S. D. Rosen. Lectin-like cell adhesion molecule 1 mediates leukocyte rolling in mesenteric venules in vivo. *Blood* 77:2553-5, 1991.

45. Lim, W.-H., W.-W. Seo, W. Choe, C.-K. Kang, J. Park, H.-J. Cho, S. Kyeong, J. Hur, H.-M. Yang, H.-J. Cho, Y.-S. Lee, and H.-S. Kim. Stent Coated With Antibody Against Vascular Endothelial-Cadherin Captures Endothelial Progenitor Cells, Accelerates Re-Endothelialization, and Reduces Neointimal Formation. *Arteriosclerosis, Thrombosis, and Vascular Biology* 31:2798-805, 2011.

46. Massia, S. P., and J. a Hubbell. Vascular endothelial cell adhesion and spreading promoted by the peptide REDV of the IIICS region of plasma fibronectin is mediated by integrin alpha 4 beta 1. *The Journal of Biological Chemistry* 267:14019-26, 1992.

47. Mellott, M. B., K. Searcy, and M. V. Pishko. Release of protein from highly cross-linked hydrogels of poly(ethylene glycol) diacrylate fabricated by UV polymerization. *Biomaterials* 22:929-41, 2001.

48. Miller, J. S., C. J. Shen, W. R. Legant, J. D. Baranski, B. L. Blakely, and C. S. Chen. Bioactive hydrogels made from step-growth derived PEG-peptide macromers. *Biomaterials* 31:3736-43, 2010.

49. Moon, J. J., M. S. Hahn, I. Kim, B. A. Nsiah, and J. L. West. Micropatterning of Poly(Ethylene Glycol) Diacrylate Hydrogels with Biomolecules to Regulate and Guide Endothelial Morphogenesis. *Tissue Engineering. Part A* 14:1-7, 2008.

50. Mutin, M., I. Canavy, a Blann, M. Bory, J. Sampol, and F. Dignat-George. Direct evidence of endothelial injury in acute myocardial infarction and unstable angina by demonstration of circulating endothelial cells. *Blood* 93:2951-8, 1999.

51. Nguyen, K. T., and J. L. West. Photopolymerizable hydrogels for tissue engineering applications. *Biomaterials* 23:4307-14, 2002.

52. Nuttelman, C. R., S. M. Henry, and K. S. Anseth. Synthesis and characterization of photocrosslinkable, degradable poly(vinyl alcohol)-based tissue engineering scaffolds. *Biomaterials* 23:3617-26, 2002.

53. Nuttelman, C. R., D. J. Mortisen, S. M. Henry, and K. S. Anseth. Attachment of fibronectin to poly(vinyl alcohol) hydrogels promotes NIH3T3 cell adhesion, proliferation, and migration. *Journal of Biomedical Materials Research* 57:217-23, 2001.

54. Padon, K. S., and A. B. Scranton. A mechanistic investigation of the three-component radical photoinitiator system Eosin Y spirit soluble,N-

methyldiethanolamine, and diphenyliodonium chloride. *Journal of Polymer Science Part A: Polymer Chemistry* 39:715-723, 2001.

55. Park, E. Y. H., M. J. Smith, E. S. Stropp, K. R. Snapp, J. a DiVietro, W. F. Walker, D. W. Schmidtke, S. L. Diamond, and M. B. Lawrence. Comparison of PSGL-1 microbead and neutrophil rolling: microvillus elongation stabilizes P-selectin bond clusters. *Biophysical Journal* 82:1835-47, 2002.

56. Park, S.-W., H.-K. Park, M.-K. Hong, S.-G. Lee, I.-S. Lee, J.-W. Kim, C. W. Lee, J.-J. Kim, and S.-J. Park. Comparison of Slotted Tube versus Coil Stent Implantation for Ostial Left Anterior Descending Coronary Artery Stenosis: Initial and Late Clinical Outcomes. *Journal of Korean Medical Science* 13:483-7, 1998.

57. Peichev, M., A. J. Naiyer, D. Pereira, Z. Zhu, W. J. Lane, M. Williams, C. Oz, D. J. Hicklin, L. Witte, M. A. S. Moore, S. Rafii, and M. C. Oz. Expression of VEGFR-2 and AC133 by circulating human CD34 + cells identifies a population of functional endothelial precursors Expression of VEGFR-2 and AC133 by circulating human CD34 ∂ cells identifies a population of functional endothelial precursors. *Blood* 95:952-958, 2000.

58. Peppas, N. A., J. Z. Hilt, A. Khademhosseini, and R. Langer. Hydrogels in Biology and Medicine: From Molecular Principles to Bionanotechnology. *Advanced Materials* 18:1345-1360, 2006.

59. Peppas, N. A., and E. W. Merrill. Development of semicrystalline poly(vinyl alcohol) hydrogels for biomedical applications. *Journal of Biomedical Materials Research* 11:423-34, 1977.

60. Rinker, K. D., V. Prabhakar, and G. a Truskey. Effect of contact time and force on monocyte adhesion to vascular endothelium. *Biophysical Journal* 80:1722-32, 2001.

61. Roger, V. L. *et al.* Heart Disease and Stroke Statistics--2012 Update: A Report From the American Heart Association. *Circulation* 125:12-230, 2011.

62. Ross, R. Atherosclerosis - An Inflammatory Disease. *The New England Journal of Medicine* 340:115-126, 1999.

63. Ross, R., and J. A. Glomset. Atherosclerosis and the Arterial Smooth Muscle Cell of smooth muscle. *Advancement Of Science* 180:1332-1339, 1973.

64. Rossi, M. L., D. Zavalloni, G. L. Gasparini, R. Mango, G. Belli, and P. Presbitero. The first report of late stent thrombosis leading to acute myocardial infarction in patient receiving the new endothelial progenitor cell capture stent. *International Journal of Cardiology* 141:e20-2, 2010.

65. Ruoslahti, E. Integrins. *Journal of Clinical Investigation* 87:1-5, 1991.

66. Ruoslahti, E. RGD and other recognition sequences for integrins. *Cancer Research* 697-715, 1996.

67. Schmedlen, R. H., W. M. Elbjeirami, A. S. Gobin, and J. L. West. Tissue engineered small-diameter vascular grafts. *Clinical Plastic Surgery* 30:507-517, 2003.

68. Schmedlen, R. H., K. S. Masters, and J. L. West. Photocrosslinkable polyvinyl alcohol hydrogels that can be modified with cell adhesion peptides for use in tissue engineering. *Biomaterials* 23:4325-32, 2002.

69. Schmidt, B. J., C. D. Paschall, W. H. Guilford, and M. B. Lawrence. High Resolution Optical Tracking to Identify Adhesive Events in Vitro. , 2007.

70. Schottelius, M., B. Laufer, and H. Kessler. Ligands for Mapping αvβ3-Integrin Expression in Vivo. *Accounts of Chemical Research* 42:969-980, 2009.

71. Scott, R. a, and N. A. Peppas. Highly crosslinked, PEG-containing copolymers for sustained solute delivery. *Biomaterials* 20:1371-80, 1999.

72. Serruys, P. W., P. D. Jaegere, and F. K. Kiemeneij. A Comparison of Balloon Expandable-Stent Implantation with Balloon Angioplasty in Patients with Coronary Artery Disease. *The New England Journal of Medicine* 331:489-495, 1994.

73. Shimizu, K., S. Sugiyama, M. Aikawa, Y. Fukumoto, E. Rabkin, P. Libby, and R. N. Mitchell. Host bone-marrow cells are a source of donor intimal smooth-muscle-like cells in murine aortic transplant arteriopathy. *Nature Medicine* 7:738-41, 2001.

74. Simper, D. Smooth Muscle Progenitor Cells in Human Blood. *Circulation* 106:1199-1204, 2002.

75. Slaughter, B. V., S. S. Khurshid, O. Z. Fisher, A. Khademhosseini, and N. A. Peppas. Hydrogels in regenerative medicine. *Advanced Materials (Deerfield Beach, Fla.)* 21:3307-29, 2009.

76. Smith, M. J., E. L. Berg, and M. B. Lawrence. A direct comparison of selectin-mediated transient, adhesive events using high temporal resolution. *Biophysical Journal* 77:3371-83, 1999.

77. Stone, G. W., J. W. Moses, S. G. Ellis, J. Schofer, K. D. Dawkins, M.-C. Morice, A. Colombo, E. Schampaert, E. Grube, A. J. Kirtane, D. E. Cutlip, M. Fahy, S. J. Pocock, R. Mehran, and M. B. Leon. Safety and efficacy of sirolimus- and

paclitaxel-eluting coronary stents. *The New England Journal of Medicine* 356:998-1008, 2007.

78. Stroncek, J. D., B. S. Grant, M. a Brown, T. J. Povsic, G. a Truskey, and W. M. Reichert. Comparison of endothelial cell phenotypic markers of late-outgrowth endothelial progenitor cells isolated from patients with coronary artery disease and healthy volunteers. *Tissue Engineering. Part A* 15:3473-86, 2009.

79. Taite, L. J., M. L. Rowland, K. a Ruffino, B. R. E. Smith, M. B. Lawrence, and J. L. West. Bioactive hydrogel substrates: probing leukocyte receptor-ligand interactions in parallel plate flow chamber studies. *Annals of Biomedical Engineering* 34:1705-11, 2006.

80. Tirtaatmadja, V. Rheology of dextran solutions. *Journal of Non-Newtonian Fluid Mechanics* 97:295-301, 2001.

81. Truskey, G. a, F. Yuan, and D. F. Katz. Transport Phenomena in Biological Systems. New Jersey, 2004.

82. Vajkoczy, P., S. Blum, M. Lamparter, R. Mailhammer, R. Erber, B. Engelhardt, D. Vestweber, and A. K. Hatzopoulos. Multistep nature of microvascular recruitment of ex vivo-expanded embryonic endothelial progenitor cells during tumor angiogenesis. *The Journal of Experimental Medicine* 197:1755-65, 2003.

83. Vickers, D. a L., and S. K. Murthy. Receptor expression changes as a basis for endothelial cell identification using microfluidic channels. *Lab on a Chip* 10:2380-6, 2010.

84. Wacker, B. K., S. K. Alford, E. a Scott, M. Das Thakur, G. D. Longmore, and D. L. Elbert. Endothelial cell migration on RGD-peptide-containing PEG hydrogels in the presence of sphingosine 1-phosphate. *Biophysical Journal* 94:273-85, 2008.

85. Weis, S., J. Cui, L. Barnes, and D. Cheresh. Endothelial barrier disruption by VEGF-mediated Src activity potentiates tumor cell extravasation and metastasis. *The Journal of Cell Biology* 167:223-9, 2004.

86. Weis, S., S. Shintani, A. Weber, R. Kirchmair, M. Wood, A. Cravens, H. McSharry, A. Iwakura, Y.-S. Yoon, N. Himes, D. Burstein, J. Doukas, R. Soll, D. Losordo, and D. Cheresh. Src blockade stabilizes a Flk/cadherin complex, reducing edema and tissue injury following myocardial infarction. *The Journal of Clinical Investigation2* 113:885-894, 2004.

87. West, J. L. Biofunctional Polymers. *Biomedical Engineering* 7:89-95, 2004.

88. West, J. L., and J. A. Hubbell. Separation of the arterial wall from blood contact using hydrogel barriers reduces intimal thickening after balloon injury in the rat:

the roles of medial and luminal factors in arterial healing. *Proceedings of the National Academy of Sciences of the United States of America* 93:13188-93, 1996.

89. Wijelath, E. S., S. Rahman, J. Murray, Y. Patel, G. Savidge, and M. Sobel. Fibronectin promotes VEGF-induced CD34 cell differentiation into endothelial cells. *Journal of vascular surgery : official publication, the Society for Vascular Surgery [and] International Society for Cardiovascular Surgery, North American Chapter* 39:655-60, 2004.

90. Williams, C. G., A. N. Malik, T. K. Kim, P. N. Manson, and J. H. Elisseeff. Variable cytocompatibility of six cell lines with photoinitiators used for polymerizing hydrogels and cell encapsulation. *Biomaterials* 26:1211-8, 2005.

91. Working, P., M. Newman, J. Johnson, and J. Cornacoff. Safety of poly(ethylene glycol) and poly(ethylene glycol) derivatives. *ACS Symposium Series* 680:45-57, 1997.

92. Yeh, E. T. H., S. Zhang, H. D. Wu, M. Körbling, J. T. Willerson, and Z. Estrov. Transdifferentiation of human peripheral blood CD34+-enriched cell population into cardiomyocytes, endothelial cells, and smooth muscle cells in vivo. *Circulation* 108:2070-3, 2003.

93. Yoder, M. C., A. C. Dudley, M. Al-latayfeh, P. S. Silva, K. Jennifer, J. A. Nagy, A. M. Dvorak, F. Harold, and W. C. Aird. Human Endothelial Progenitor Cells. *Cold Spring Harbor Perspectives in Medicine* 1-14, 2011.doi:10.1101/cshperspect.a006692

94. Yoder, M. C., L. E. Mead, D. Prater, T. R. Krier, K. N. Mroueh, F. Li, R. Krasich, C. J. Temm, J. T. Prchal, and D. a Ingram. Redefining endothelial progenitor cells via clonal analysis and hematopoietic stem/progenitor cell principals. *Blood* 109:1801-9, 2007.

APPENDIX A

PEG Acrylation Sample Calculations

$$MW_{PEGmonomer} = 44.053 g/mol$$

$$MW_{PEG} = 6000 g/mol$$

$$n_{monomer} = \frac{MW_{PEG}}{MW_{PEGmonomer}} = \frac{6000}{44.053} = 136.2$$

$$n_{proton/monomer} = 4$$

Integrated intensity of PEG peak

$$(I_{PEG}) = 268.08$$

Integrated intensity of acrylate single proton peaks

$$I_{acrylate1}, I_{acrylate2}, I_{acrylate3} = 0.970, 0.920, 0.960$$

$$n_{PEG} = \frac{I_{PEG}}{n_{proton/monomer} \times n_{monomer}} = \frac{I_{PEG}}{4 \times 136.2} = 0.492$$

$$n_{tacrylate} = n_{PEG} \times 2 = 0.492 \times 2 = 0.984$$

$$n_{acrylate} = \frac{I_{acrylate1} + I_{acrylate2} + I_{acrylate3}}{3} = \frac{0.970 + 0.920 + 0.960}{3} = 0.950$$

Acrylation percentage

$$= \frac{n_{acrylate}}{n_{tacrylate}} \times 100\% = \frac{0.950}{0.984} \times 100\% = 96.5\%$$

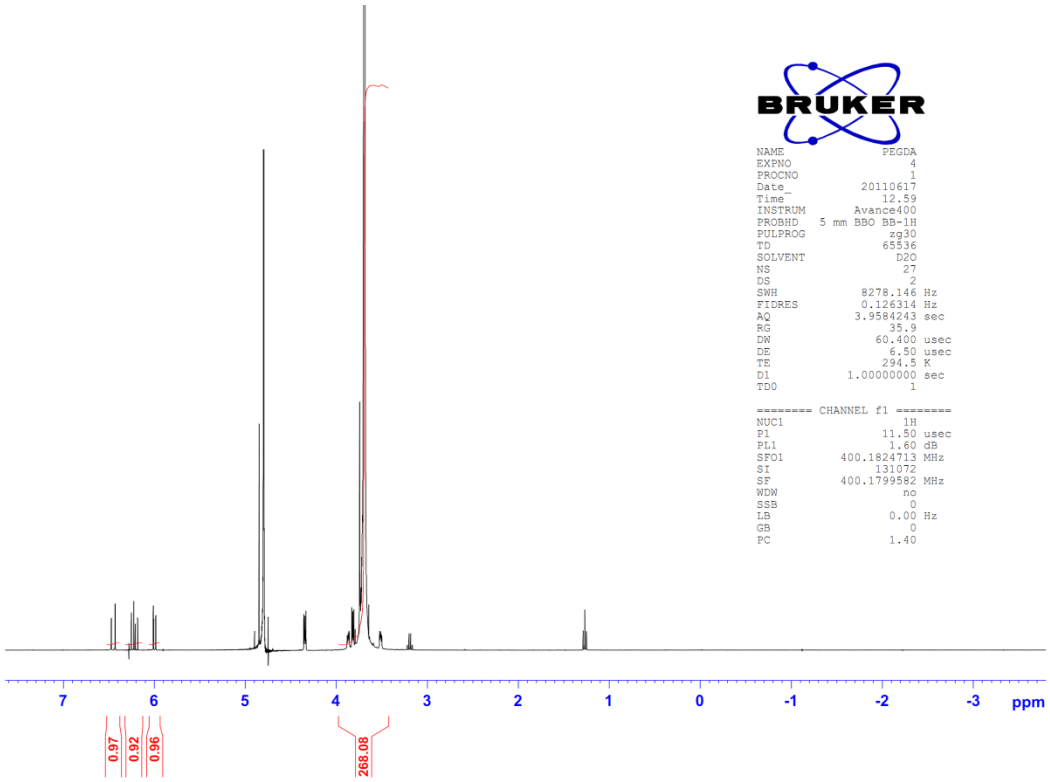

Figure 38: NMR diagram showing the integrated intensity of protons on acrylate groups and PEG of PEGDA chain.

APPENDIX B

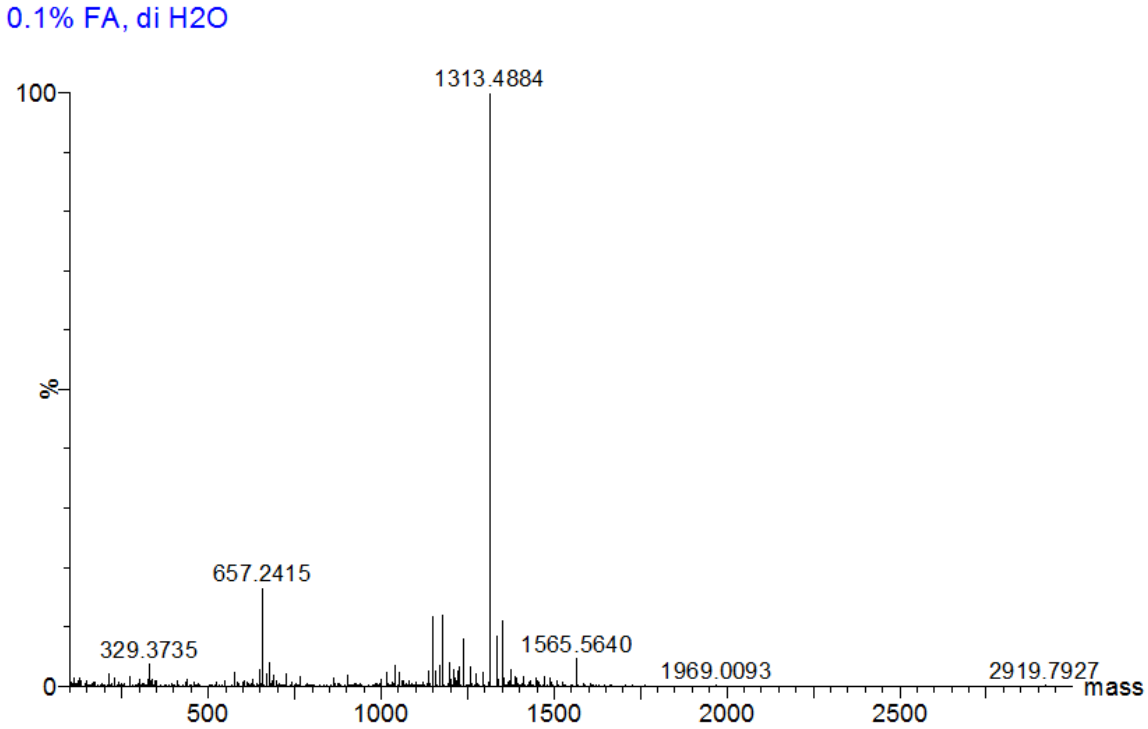

Figure 39: Confirmation of the mass of 6HRGDS by mass spectrometry. The peak 1313.4884 represented the protonized 6HRGDS which has a MW of 1312.556.

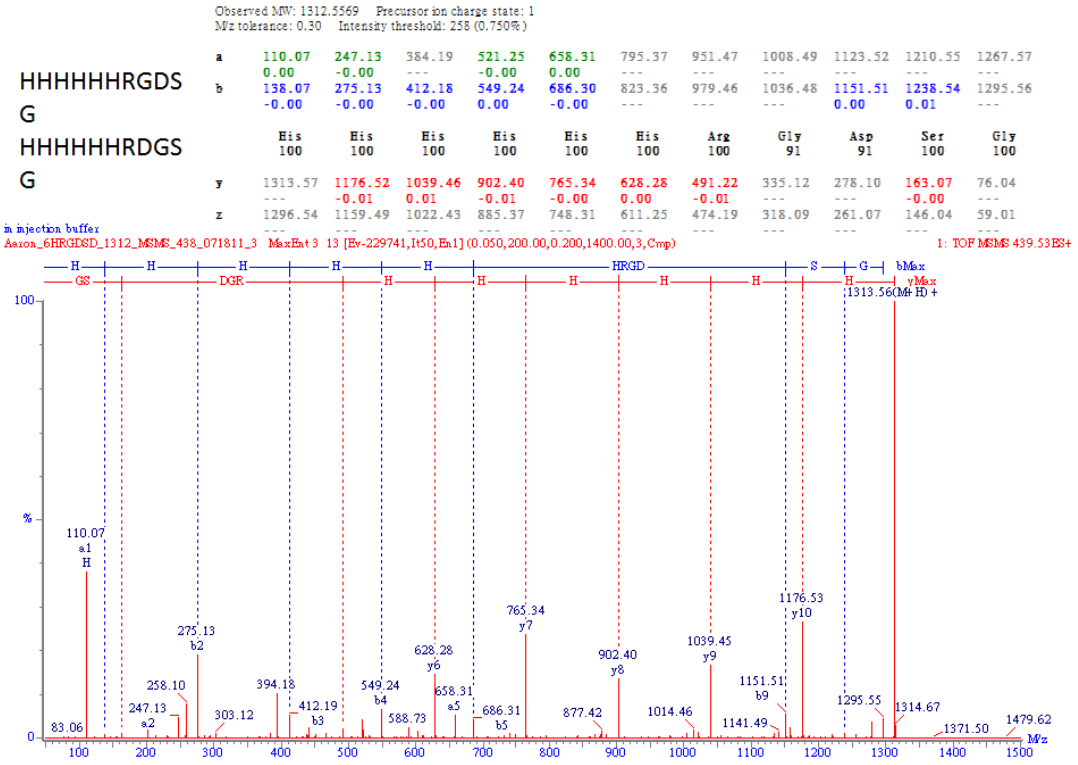

Figure 40: Sequencing result showing that the peptide HHHHHHRGDS was synthesized.